REFERENCE
NBS PUBLICATIONS
NAT'L INST. OF STAND & TECH
A11106 031716

NBSIR 85-3131

Laboratory Design and Test Procedures for Quantitative Evaluation of Infrared Sensors to Assess Thermal Anomalies

Y. May Chang
Richard A. Grot

U.S. DEPARTMENT OF COMMERCE
National Bureau of Standards
National Engineering Laboratory
Center for Building Technology
Gaithersburg, MD 20899

James T. Wood

DCS Corporation
Alexandria, VA 22314

June 1985

Prepared for:
Office of Building Energy Research and Development
U.S. Department of Energy
Washington, DC 20585

QC
100
.U56
85-3131
1985

NATIONAL BUREAU
OF STANDARDS
LIBRARY
QC 100 .U56 NBSIR 85-3131 1985

NBSIR 85-3131

LABORATORY DESIGN AND TEST PROCEDURES FOR QUANTITATIVE EVALUATION OF INFRARED SENSORS TO ASSESS THERMAL ANOMALIES

Y. May Chang
Richard A. Grot

U.S. DEPARTMENT OF COMMERCE
National Bureau of Standards
National Engineering Laboratory
Center for Building Technology
Gaithersburg, MD 20899

James T. Wood

DCS Corporation
Alexandria, VA 22314

June 1985

Prepared for:
Office of Building Energy Research and Development
U.S. Department of Energy
Washington, DC 20585

U.S. DEPARTMENT OF COMMERCE, Malcolm Baldrige, *Secretary*
NATIONAL BUREAU OF STANDARDS, Ernest Ambler, *Director*

ABSTRACT

This report presents the description of the laboratory apparatus and preliminary results of the quantitative evaluation of three high-resolution and two low-resolution infrared imaging systems. These systems which are commonly used for building diagnostics are tested under various background temperatures (from -20°C to 25°C) for their minimum resolvable temperature differences (MRTD) at spatial frequencies from 0.03 to 0.25 cycles per milliradian. The calibration curves of absolute and differential temperature measurements are obtained for three systems. The signal transfer function and line spread function at ambient temperature of another three systems are also measured. Comparisons of the dependence of the MRTD on background temperatures from the measured data with the predicted values given in ASHRAE Standards 101-83 are also included. The dependence of background temperatures for absolute temperature measurements are presented, as well as comparison of measured data and data given by the manufacturer. Horizontal on-axis magnification factors of the geometric transfer function of two systems are also established to calibrate the horizontal axis for the measured line spread function to obtain the modulation transfer function. The variation of the uniformity for horizontal display of these two sensors are also observed. Included are detailed descriptions of laboratory design, equipment setup, and evaluation procedures of each test.

Key words: Background temperature; calibration curves; display uniformity; infrared sensing systems; laboratory evaluation; line spread function; magnification factor; minimum resolvable temperature difference; modulation transfer function; signal transfer function; spatial frequency; target temperature.

TABLE OF CONTENTS

PAGE

Abstract.....iii

List of Tables.....vii

List of Figures.....viii

1. Introduction.....1

2. Description of Evaluation Facility.....3

3. Quantitative Evaluation of Infrared Thermographic Sensors---
Procedures and Results.....7

3.1 Minimum Resolvable Temperature Difference (MRTD).....7

3.2 Temperature Calibration Curves.....10

3.3 Signal Transfer Function (SiTF).....12

3.4 Optical Transfer Function (OTF).....14

3.5 Geometric Transfer Characteristics.....16

3.6 Display Uniformity.....17

4. Conclusions.....18

5. Acknowledgements.....19

6. References.....20

Tables.....22

Figures.....33

Appendix.....A-1

LIST OF TABLES

Table 1. Specification of Building Diagnostic Sensors

Table 2. Instrument Items for the Evaluation Facility

Table 3. Test Target Sizes Required for Building Diagnostic Sensors

Table 4. Parameters Evaluated for Each Infrared System

Table 5. Checklist for MRTD Testing of Sensors

Table 6. Parameters Determined from Absolute Temperature Measurements

Table 7. Checklist for SiTF Testing of Sensors

Table 8. Temperature Windows from SiTF Tests

Table 9. Temperature Shifts from SiTF Tests

Table 10. Checklist for OTF Testing of Sensors

Table 11. Measurements and Results from On-Axis Magnification Test

Table 12. Results from Uniformity Test

LIST OF FIGURES

Figure 1. Overall Facility Concept

Figure 2. Basic Configuration for Test Sensor with Eyepiece

Figure 3. Basic Configuration for Test Sensor with Remote Display Monitor

Figure 4. Overall Facility Setup for Imaging Systems with Eyepiece

Figure 5. Overall Facility Setup for Imaging Systems with Remote Display Monitor

Figure 6. Target Patterns Used for Various Tests

Figure 7. Minimum Resolvable Temperature Difference (MRTD) Test Pattern in Target Module

Figure 8a. Minimum Resolvable Temperature Difference (MRTD) versus Spatial Frequency at Various Background Temperatures T of System A (S=2)

Figure 8b. Minimum Resolvable Temperature Difference (MRTD) versus Spatial Frequency at Various Background Temperatures T of System B (S=5)

Figure 8c. Minimum Resolvable Temperature Difference (MRTD) versus Spatial Frequency at Various Background Temperatures T of System C (S=10)

Figure 8d. Minimum Resolvable Temperature Difference (MRTD) versus Spatial Frequency at Various Background Temperatures T of System D

Figure 8e. Minimum Resolvable Temperature Difference (MRTD) versus Spatial Frequency of Systems A, B, C, D, and E (Blackground Temperature T $\simeq$ 23°C)

Figure 9a. Minimum Resolvable Temperature Difference (MRTD) versus Background Temperature of System A (S=2) for the Two ASHRAE Specified Test Frequencies

Figure 9b. Minimum Resolvable Temperature Difference (MRTD) versus Background Temperature of System B (S=5) for the Two ASHRAE Specified Test Frequencies

Figure 9c. Minimum Resolvable Temperature Difference (MRTD) versus Background Temperature of System C (S=10) for the Two ASHRAE Specified Test Frequencies

Figure 9d. Minimum Resolvable Temperature Difference (MRTD) versus Background Temperature of System D for the Two ASHRAE Specified Test Frequencies

Figure 10. Image Display of System C for Pattern #4 at Background Temperature of -17°C

Figure 11a. Factor of Decrease for the Instrument Sensitivity Versus Object Temperature of Systems A and D (Using 30°C as Reference)

Figure 11b. Factor of Decrease for the Instrument Sensitivity Versus Object Temperature of Systems B and C (Using 30°C as Reference)

Figure 12a. Absolute Temperature Calibration Curves of System A at Various Background Temperatures T (S=2, Aperture = f/1.8)

Figure 12b. Absolute Temperature Calibration Curves of System B at Various Background Temperatures T (S=2, Aperture = f/1.8)

Figure 12c. Absolute Temperature Calibration Curves of System C at Various Background Temperatures T (S=10)

Figure 13a. Differential Temperature Calibration Curves of System A at Various Background Temperatures T (S=2)

Figure 13b. Differential Temperature Calibration Curves of System B at Various Background Temperatures T (S=2)

Figure 13c. Differential Temperature Calibration Curves of System C at Various Background Temperatures T (S=10)

Figure 14. Instrumentation Setup for Signal Transfer Function (SiTF) Tests

Figure 15a. Relative Brightness versus Temperature Difference from SiTF Test of System A at Constant Thermal Level (TL=26.5) for Various Gains

Figure 15b. Relative Brightness versus Temperature Difference from SiTF Test of System B at Constant Thermal Level (TL=54) for Various Gains

Figure 15c. Relative Brightness versus Temperature Difference from SiTF Test of System D at Maximum Thermal Level (Brightness) for two gains (Contrast)

Figure 15d. Relative Brightness versus Temperature Difference from SiTF Test of System A at Constant Gain (S=2) for Various Thermal Levels

Figure 15e. Relative Brightness versus Temperature Difference from SiTF Test of System B at Constant Gain (S=5) for Various Thermal Levels

Figure 16a. Line Spread Function (LSF) of System A as a Function of Distance in Object Space (S=2, TL=26, and $\Delta T=18^{o}C$)

Figure 16b. Line Spread Function (LSF) of System B as a Function of Distance in Object Space (S=2, TL=54, and $\Delta T=15^{o}C$)

Figure 17a. Modulation Transfer Function (MTF) of System A as a Function of Object Space Frequency (S=2, TL=26, and $\Delta T=18^{o}C$)

Figure 17b. Modulation Transfer Function (MTF) of System B as a Function of Object Space Frequency (S=2, TL=54, and $\Delta T=15^{o}C$)

1. INTRODUCTION

Over the past decade, infrared technology has been widely used as a diagnostic tool to assess thermal anomalies in building envelopes. Thermal patterns produced by the infrared imaging systems provide rapid and useful information on thermal performance of structures, and can be used to analyze the heat loss and overall energy efficiency of buildings [1]. Due to the complex and transient nature of heat flow through structures, it is critical for the users to know the accuracy and parameters of their equipment in order to assess the accuracy of their measurements. Manufacturers of infrared sensing devices often give specifications in their operating manuals and procedures for calculating temperature measurement corrections from the given parameters, such as sensitivity, thermal ranges, isotherm levels, etc [2]. These parameters are not sufficient to determine the overall performance of the equipment. A good example is the temperature dependence under various environmental conditions. When using the infrared imaging systems for building inspections, the difference between interior and exterior air temperatures should be large enough to create enough heat flow for accurate inspections. This implies that the colder the outside temperature is, the more accurate the measurement should be. However, for exterior inspections, as the outside air temperature decreases, the sensitivity of instruments falls off much faster than the increase of heat flow. As a result, the thermal image produced by some sensing equipment under extremely cold outside temperature will show no contrast [3].

Due to the fact that manufacturers have no standard specifications for characterizing performance of infrared imaging systems, it is difficult to predict the performance of sensing devices in building diagnostic applications. For example, "thermal sensitivity" sometimes is defined as the minimum resolvable temperature difference (MRTD) at some unknown spatial frequency, while other times it is described as MRTD with no reference to frequency, or even is given as noise-equivalent temperature difference (NETD)*. Further, there is no laboratory facility available in the USA to calibrate infrared imaging systems and to compare their performance for building diagnostic purposes. Therefore, it becomes necessary to test such equipment under various temperature conditions prior to its use for building diagnostic purposes. In general, the image evaluation parameters which are meaningful for system specifications are: 1) summary measurements; 2) signal transfer characteristics; 3) geometric transfer characteristics; 4) spatial resolution; and 5) noise characteristics. The first parameter involves human interpretation of the image display of the sensor, and hence is

---

* NETD is defined as the blackbody target-to-background temperature difference in a standard test pattern which produces a signal-to-noise ratio of unity.

the most critical factor, when the image is used for qualitative measurements. In building diagnostic applications, the most important summary measure is the MRTD which determines the ability of an imaging system to detect thermal anomalies in building envelopes.

Accordingly, the infrared image facility at the National Bureau of Standards (NBS) was designed to test and evaluate infrared imaging devices used in building inspections [4]. The parameters which are needed for evaluating the performance of an infrared sensor* are: 1) the minimum resolvable temperature difference (MRTD), which measures the capability of the compound observer-imaging system to distinguish well-defined bar patterns on the display as a function of temperature difference between target and background; 2) the signal transfer function (SiTF), which measures the signal gain of the sensor as a function of brightness and gain controls and calibrates the dynamic range of measurement windows; 3) the optical transfer function (OTF), which measures the spatial resolution of a sensor based on the Fourier Transform of the line spread function; 4) the geometric transfer function, which measures the variation in local magnification of a sensor across the horizontal field-of-view (FOV)**; and 5) the display uniformity of the detector, which measures the variations in brightness across the display when the sensor is viewing a uniform-temperature target. The functions that the image evaluation laboratory is facilitated to perform include: 1) determination of the parameters of sensors, 2) comparison of the performance among candidate sensors, 3) diagnosis of problems in available sensors, 4) evaluation of new technology sensors, and 5) service as a central standard facility for the building diagnostic community. In addition, the calibration curves for absolute target temperatures as well as differential temperatures at various conditions are generated. Detailed description of the evaluation facility, test procedures, and test results for instruments are discussed in the following sections.

---

* In this report, a sensor is equivalent to an imaging system.

** FOV is defined as the total angular dimensions with which objects can be imaged, recorded, and displayed by a sensor when pointed in a fixed direction.

2. DESCRIPTION OF EVALUATION FACILITY

The NBS infrared imaging evaluation (IE) facility which was designed by the DCS corporation* under specifications by researchers at NBS is dedicated to calibrate, evaluate, and compare sensing devices presently on the market for building diagnostics [4]. Based on the documents in ASHRAE [5-7] and ASTM [8-9] standards, and the choice of various characteristics, seven sensors were originally selected as samples to be tested. Table 1 gives the summarized principle characteristics of these selected sensing devices which are currently available or are expected to be available in the near future with specifications for building diagnostics. One of the existing environmental chambers at NBS, whose dimensions are approximately 3m wide x 3m high x 6m long, is utilized to provide ambient temperature simulated to actual field conditions. The temperature range of the chamber is from -20°C to 60°C (0°F and 140°F). The control room adjacent to the chamber is used to control the temperature of the chamber, the blackbody source and the remote monitor display, except for sensors that use an eyepiece instead of remote monitor display. For these sensors, the observer remains in the chamber.

The schematic of the overall facility is shown in figure 1. At present, the instrumentation setup is complete except for a computer-controlled interface which is intended to be installed in the future. The equipment required for the evaluation facility was either purchased or constructed by the NBS machine shop. Table 2 is a list of instruments that are required. Detailed drawings of the hardware that were custom built by NBS are contained in the appendix.

The ASHRAE and ASTM standards which are to be satisfied by the test facilities are summarized below:

- The accuracy of differential temperature measurement between source and background must be less than 0.1°C.
- The accuracy of source absolute temperature measurement must be 1°C.
- The distance between the target and the sensor must be sufficient for the field of view of the sensor to subtend a minimum area of 0.8m wide x 0.6m high in object space.
- The MRTD test must include equivalent pattern sizes of 0.52 and 0.13 cycles/cm, for class A and class B surveys, respectively.

---

* Such identification does not imply recommendation or endorsement by the Nationsl Bureau of Standards.

- The accuracy of luminance measurement of the display must be sufficient to easily determine a shade of grey variation.

- Controlled environment must be able to relate to and validate exterior measurement capabilities of sensors.

From the specifications of typical commerically available sensors listed in table 1 further requirements of the characteristics of sensors as well as other instruments of the NBS laboratory facility are:

1) The blackbody source must be able to produce significant temperature differences of 0.02°C, in order to test the quoted sensitivity for sensors and to be consistent with the standards.

2) By using multiple objective lens configurations with the imaging sensors to obtain approximately 20° horizontal FOV, the ASHRAE/ASTM required test target sizes and distances between targets and sensors were generated as given in table 3. Table 3 shows that all systems will fit within a 6m long chamber, if they are required to meet the ASHRAE/ASTM MRTD test and field of view constraints for interior survey work (to cover minimum area of 0.8m wide x 0.6m high). Furthermore, the requirement for a class B pattern, stated in ASHRAE/ASTM Standards, can also be fit to a 13.5cm x 13.5cm aperture on the heat source if everything is scaled down by a factor of two. There may be some focusing problems for sensors which can be adjusted to a closer than publicized near-focus distance.

3) The output coupling optics for making any measurements from the display requires a compatibility to both infinite conjugate (eyepiece) and finite conjugate (remote monitor) displays. This is due to the fact that images from sensors with eyepieces are either on a miniature 2.54cm CRT display or real images of an LED array while those from sensors with remote displays are on CRT for direct viewing.

4) The platforms must be able to handle weights up to 12 kg.

The basic configuration of major components of the laboratory facility to test sensors with an integrated eyepiece can be broken down into modules as illustrated in figure 2. Figure 3 is a similar setup for testing sensors with remote displays. (Note that all units, as well as display monitors are outside the chamber.) According to figures 2 and 3, there are three modules which contain 23 items for the laboratory setup:

1) Target/Source pattern module (which includes items 1-8):

Items 1-4: target/source table with mounting plate to position target and background plate

Item 5: blackbody source to provide target radiation

Item 6: temperature controller for blackbody source to indicate target, background, and differential temperatures

Item 7: background plate

Item 8: target pattern holder.

2) Image sensor position module (which includes items 9-12 and 20):

Sensor/monitor table with mounting plate to position sensor for viewing the target with horizontal, vertical, and rotational movement capabilities.

3) Display monitor module (which includes items 13-19 and 21-23):

To measure relative brightness from the sensor's display, mounted outside or inside of the chamber.

Item 13: coupling lens to transfer image from the display to the radiometric probe

Item 14: optical rail to be mounted external to the chamber (when testing sensors with remote displays) or internal to the chamber (when testing sensors with integrated eyepieces)

Item 15: radiometric scanning eyepiece to scan signal from display

Item 16: fiber optic cable to transfer light energy to the photomultiplier tube

Item 17: photomultiplier tube (PMT) whose output is being monitored

Items 18-19: digital radiometer with motor drive for scanner to monitor signals from PMT

Items 21-23: remote monitor display table with mounting plate and block to position monitor with horizontal, vertical, and rotational movement capability.

Future installation of a data analysis module is intended to provide power to drive the facility components to various positions. This module would also be capable of manipulating output signals and presenting them in various formats and making further calculations. Figures 4 and 5 are photographs to show the overall facility setup at NBS for imaging systems with integrated eyepiece and with remote monitors, respectively.

Among the selected infrared sensing equipment, only systems A and B are properties of NBS. Quantitative evaluation of these two systems has been completed. Due to the constraint of scheduling, only partial measurements were made on some systems, and due to unavailability, no test measurements were made on two systems. Table 4 indicates the parameters that were evaluated for each infrared sensing device.

3. QUANTITATIVE EVALUATION OF INFRARED THERMOGRAPHIC SENSORS--PROCEDURES AND RESULTS

3.1 Minimum Resolvable Temperature Difference (MRTD)

This important test evaluates the capability of the compound imaging system-observer to resolve a well-defined bar target on the display monitor at various temperature difference between target and background (ΔT). It is used in both the ASHRAE standard 101-83 [7] and the proposed ASTM standard practice for inspecting thermal defects in cavity wall insulation installations [9]. By definition, the MRTD of a sensing device is the lowest ΔT at which the pattern in a standard periodic 4-bar pattern with aspect ratio of 7:1 is resolvable by observers as a 4-bar pattern. During the test, there are no limits on viewing time and no restrictions on thermal level and gain controls. The MRTD is a function of both the spatial frequency of the bar pattern and the ambient temperature of the background reference. The ASTM and ASHRAE standards have specifications on minimum distance (1 meter) between the target and the sensor, and minimum FOV (varies for individual sensors) for infrared imaging systems. Accordingly, the distance between the sensor and the target for each system is determined. Table 5 is a checklist for the MRTD test for various imaging systems. Figure 6 shows all target patterns constructed. Patterns #1 to #5, with target spatial frequencies of 0.26, 0.52, 0.75, 1.04, 1.25 cycles/cm, respectively are used for the test. Figure 7 shows one of the patterns mounted in the target module. The source and background plates must be matched with emissivities above 0.95 and have controllable and measurable temperature difference below 0.02°C. The imaging system is aligned with the target/background so that the bar direction is perpendicular to the scan direction, and the displayed image is centered and in sharp focus, using $\Delta T = 5°C$ and pattern #5, which is near the limit of resolution.

The procedure is to start with pattern #1, a very low input frequency pattern, and a negative ΔT of magnitude great enough to result in an image with four black bars. The observer increases the ΔT in small increments (less than 0.1°C) until the four black bars can no longer be distinguished from the background. This value of $\Delta T = \Delta T1$ is recorded. The observer increases ΔT until the four black bars first appear as white and records the value of $\Delta T = \Delta T2$. The MRTD, for this particular spatial frequency, is defined as the mid-point of these ΔT's, i.e. $MRTD = (1/2)\cdot(\Delta T2 - \Delta T1)$. The brightness (level) and gain (contrast) control settings of the sensor are also documented. The same measurements are repeated for successively higher spatial frequencies, patterns #2 to #5, to obtain the MRTD for each pattern with brightness and gain controls remaining at the same positions. If more than one person runs the test, the results are averaged. Since the MRTD is often a function of background temperature, the same test should be run by decreasing the chamber temperature, from room temperature ($\simeq$25°C), to obtain data sets as a function of temperature. As previously

prescribed, the control room outside of the chamber is utilized to control the blackbody source temperature as well as the display for such imaging systems with remote monitors. As for sensors with integrated eyepieces, the entire setup is inside the chamber.

Five infrared sensing systems were evaluated for their MRTD characteristics, of which three are high-resolution imaging systems (HRIS A, B, and C) with remote display monitors, and two are low-resolution imaging systems (LRIS D and E) with eyepiece displays. These systems are all commonly used for building inspections and their specifications are given in table 1. The results of the MRTD tests are illustrated in figures 8a to 8e and 9a to 9d.

Figures 8a to 8e show the MRTD versus spatial frequency of systems A, B, C, and D at various ambient temperatures and a comparison of all five systems at room temperature. The expected MRTD versus spatial frequency curve is such that at low spatial frequencies the curve is fairly level and approaches the minimum detectable temperature difference (MDTD)* of the system and at some higher spatial frequency, there is a spatial frequency at which the curve becomes asymtotically vertical. Above this frequency, the imaging system cannot be used to detect anomalies. All systems exhibit this behavior, as shown in figures 8a to 8e.

System A indicates a stronger spatial frequency dependence than systems B and C. As shown in figure 8a, at room temperature of 25°C, the MRTD of system A increases from 0.04°C, at the spatial frequency of 0.03 cycles per milliradian, to 0.7°C, at a spatial frequency of 0.15 cycles per milliradian. Figure 8b illustrates that the MRTD of system B at 22°C room temperature at the same spatial frequencies are 0.04°C and 0.4°C, respectively. As for system C, the MRTD's observed at these spatial frequencies at 23°C room temperature are 0.05°C and 0.2°C, respectively as shown in figure 8c. Further, no asymptotic tendencies are noted at the higher spatial frequencies of the MRTD curve for system C at this ambient temperature (23°C). The MRTD curve at ambient temperature of -7°C shows a slight tendency of a vertical asymptote. However, when the ambient temperature dropped to -15°C and below, the image display from system C of the bar patterns has some type of distortion, as shown in figure 10, such that no clear image can be observed to determine the MRTD. Sources of such phenomenon, due to either the limitation of instrumentation or defectiveness of instrumentation during tests are not clear. The MRTD curves of systems A and B seem to become vertical at a frequency slightly greater than 0.16 cycles per milliradian, while the MRTD curves of system C indicate they are still increasing monotonically at 0.16 cycles per milliradian. Therefore, the limiting spatial frequency of system C cannot be estimated without testing this system at higher spatial frequencies.

---

* MDTD is similar to MRTD except the target is a specified square of uniform temperature distribution instead of 4-bar patterns.

Figure 8d shows that the MRTD's of system D are higher than systems A, B, and C and its limitation to detect anomalies is at approximately 0.27 cy/mrad. Test results of system E indicate that it has lower MRTD's than systems A, B, C and D at the high spatial frequency range, as illustrated in 8e. At the low spatial frequency range, the MRTD's of this LRIS seem to be slightly higher than those of the HRIS. This implies that system E under test at ambient temperatures of 24°C has better ability to resolve temperature differences between sources and their background for small objects than the other systems.

The temperature dependence of the MRTD of these HRIS's are shown in figures 9a to 9d at the two spatial frequencies specified by the ASHRAE standards. The MRTD for each imaging system increases as the ambient temperature of the chamber drops which implies that, for exterior inspections, the instrument sensitivities will fall off as the outside temperature decreases. For example, figure 9c illustrates that system C will not detect bar pattern #4 at a chamber temperature below -12°C and bar pattern #1 below -18°C. The ASHRAE standard describes a theory developed to explain this phenomenon of the MRTD [7]. From this theory a factor of decrease can be calculated for the instrument sensitivity when the infrared sensing device is used at an object temperature below 30°C, the reference temperature. However, using data from the laboratory measurements, the factor of decrease for MRTD at various ambient temperatures below 30°C can be obtained graphically. Since the values of temperature difference (MRTD) are small (<1°C) except using system D for detecting pattern #4, the object temperature and background temperature can be considered as the same value. The measured and the theoretical factors of decrease are superimposed in figures 11a and 11b. The factor of decreasing sensitivity curves in figures 11a and 11b for systems A, B, and C are using the average values observed from patterns #1 and #4, and for system D is using data from pattern #1 only. By comparing the results of systems with short wavelength (with spectral range from 3 to 5.6 um), as illustrated in figure 11a, it can be seen that the measured instrument sensitivity of system A agrees quite well with the ASHRAE's calculated values. Figure 11a also indicates that system D has better instrument sensitivity than that from ASHRAE calculation [7], but the measured data are for detecting low frequency pattern #1 only and they probably do not represent its sensitivity for observing all spatial frequencies. By comparing the results of systems with long wavelength (with spectral range from 8 to 14 um), as shown in figure 11b, the measured instrument sensitivity of system B is slightly lower than the ASHRAE calculated values except at extremely low environmental temperatures (≤-17°C), where its sensitivity falls off much faster . As for system C, its measured sensitivity was found to be much lower than that from the ASHRAE theoretical calculations at temperatures lower than 2°C. One possibility of this discrepency in the behavior of system C with respect to the ASHRAE theory may be attributable to the design of the unit which is not accounted for by the emitted radiation theory assumed in the ASHRAE standards.

3.2 Temperature Calibration Curves

By using infrared equipment for temperature measurement, the numerical data received from the thermal radiation of an object is often called the thermal value or thermal level in isotherm units (IU), indicated on the front panel of the instrument. The relationship between the thermal value and the object temperature is non-linear and is sometimes given by the manufacturer as graphical curves. Accordingly, the quantitative temperature of an object can be obtained from the absolute temperature calibration curves, which describe the relationship of object temperature and the instrument's thermal level and the thermal value. This calibration curve can be generated by using a square pattern of 5.1 cm x 5.1 cm and the blackbody source to produce accurate target temperatures from below ambient to above ambient temperatures. The adjustment of isotherm controls will give the isotherm units of the thermal level by brightening the target image. (Detailed procedures are given by individual manufacturers). In our laboratory experiment, the absolute temperature calibration curves are generated at various ambient temperatures, while the curves or data given by manufacturers are often tested at room temperature of approximately 20°C. As a result, besides checking manufacturer's calibration curves, temperature dependence of the infrared system for absolute temperature measurement can also be established.

The results of this test for the three HRIS (systems A, B, and C) at various chamber temperatures are shown in figures 12a to 12c. The relationship between thermal value (in IU) and object temperature for systems A and B is given by the manufacturers in eq. (1).

$$I = \frac{A}{C \cdot \exp(B/T) - 1} \qquad (1)$$

where I is the thermal value in IU corresponding to T,
T is the object temperature in degree Kelvin (°K),
and A, B, and C are calibration constants for the settings of the instrumentation.

Absolute temperature calibrations for system A were measured at ambient temperatures from -20°C to 24°C, and they agree with the calibration curve given by the manufacturer, which was generated at a sole room temperature. Data points in figure 12a are from measurements of three background temperatures, -20°C, -1°C, and 20°C, and from the comparison of these curves they do not show any temperature dependence. The calibration curve from laboratory measurements is determined by fitting the entire data set to eq. (1) using regression analysis. However, absolute temperature measurements from systems B and C do not have the same behavior. System B was tested from -19°C to 25°C ambient temperature. Data points in figure 12b are measurements of system B at background temperature -19°C, 1°C, and 25°C, and they

indicate a strong dependence on background temperatures and exhibit noticeable temperature shifts from the manufacturer's curve (tested at 22°C), especially at low ambient temperatures. Data points at each background temperature were fitted to eq. (1), as shown by dotted lines in figure 12b. Table 6 gives the parameters from the manufacturer and those obtained by fitting measured data of systems A and B to eq. (1). Note that these two systems were tested for more than three ambient temperatures and figures 12a and 12b only contain data for three temperatures. Absolute temperature measurement dependence on background temperature for system C is only observed at low ambient temperatures, such that a significant temperature shift is observed from -1°C to -20°C and only a slight variation from 23°C to -1°C, also shown in figure 12c. This may be due to a limitation of the system and related to the distortion observed in MRTD test at low ambient temperatures. Also note that the curve for system C is the relationship between the dial setting of thermal level (rather than isotherm units) and object temperature, which give lower values at high object temperatures, as shown in figure 12c.

Another test of temperature calibration curves that can be done is the temperature differential versus isotherm difference at various environmental temperature conditions. This is useful for many applications that require only differential temperatures. This test also uses the 5.1 cm x 5.1 cm square pattern. By changing the temperature difference of target to background (ΔT) at a constant thermal level, the isotherm difference corresponding to each ΔT can be measured. The same test should be run at various ambient temperatures to establish the system's temperature dependence in measuring temperature differences.

The results of the differential temperature measurement for systems A, B, and C at ambient temperatures from -20°C to 25°C are shown in figures 13a to 13c. All systems have linear responses of isotherm difference versus temperature difference with the slopes related to the background temperatures. These straight lines in figures 13a to 13c are determined by linear regression for each data set, and the regression lines of fitting the entire data set for each system are also included.

3.3 Signal Transfer Function (SiTF)

The purpose of this test is to verify and calibrate the dynamic range of the sensors being used for thermography by measuring their signal gain as a function of brightness and gain controls. The curves generated from the SiTF test describe the output luminance of a device at low spatial frequency as a function of the input target signal (ΔT) over the entire operating range. The data from this test is obtained by increasing the input target temperature differential from below ambient to a ΔT where the system reaches saturation. As a result, the temperature window for the contrast (gain) setting and the characteristics of temperature shifting from level (brightness) control of an imaging system can be established.

The target pattern used for SiTF test is a 5.1 cm x 5.1 cm square aperature whose area subtends approximately 1% of the field of view (FOV) of the sensors under test. The background plate should fill the remainder of the FOV and combine with the blackbody source of high emissivity. Figure 14 shows the instrumentation setup for the SiTF test. A photometric probe whose projected size is large compared to a scan line and small enough to fall completely within the image aperature is used in the Receiver Module to monitor the output luminance. Table 7 is a checklist for the SiTF test for various imaging systems.

The test is conducted in the following way. Initially, with pattern #6 (5.1 cm x 5.1 cm square) in position and the differential temperature of source to background (ΔT) equal to 5°C, adjust the target/background and sensor/monitor tables at a distance according to table 7 and center the imaging of the target on display. Prior to mounting the optical rail (item 14), focus the image of the aperture target until it is sharp to the eye. Mount the radiometric probe and the coupling lens as one module on the optical rail, and make fine adjustment on this module to position the probe aperture in the center of the square target image. Next, cover the radiometric probe as well as the coupling lens with heavy black cloth to reduce stray light. The photomultiplier tube (PMT) and the digital radiometer should be setup according to the manufacturer's recommendation and to give an output signal well below the maximum when the brightness of the display is at saturation. Generate SiTF by adjusting the blackbody source from a negative temperature difference (ΔT equals about -5°C) to a value at which the output signal is saturated. Record both values of ΔT's and relative brightness output from the radiometer. Repeat the similar measurement for various combinations of brightness (level) and gain (contrast) settings of the sensor by using approximately three settings (maximum, mid-point, and minimum) of each. Therefore, the SiTF of different gains at a fixed brightness, and various brightness at a constant gain are measured.

The results from the SiTF test for systems A, B, and D are shown in figures 15a to 15c which illustrate the relative brightness

from the radiant as a function of the temperature difference between the background and the target of these three systems. System A was tested at thermal levels in isotherm units (IU) of 22, 26.5, and 28 with gain settings at S=2, S=5, and S=10. System B was tested at thermal levels of 50, 54, and 56 with gain settings at S=2, S=5, and S=10. System D, which does not have any marked settings, was tested at approximately maximum and midpoint of contrast with maximum brightness. When testing system D at brightness setting less than the maximum and the contrast setting at minimum, the output signals failed to reach saturation even with ΔT greater than 15°C.

The linear regions of these SiTF curves are determined by using linear regression analysis. Number of data points as a function of goodness of fit is compared to fit data at the most points of each curve. The temperature windows corresponding to each contrast setting at various thermal levels can be established from the regression line as it goes from 1% to 90% of the maximum brightness (at saturation) of the SiTF curve. The linear region of temperature shifts from changing thermal levels can be obtained from the shifts at the midpoint of these regression lines for each contrast setting. The results of the temperature windows and temperature shifts for the imaging systems are given in tables 8 and 9.

Table 8 shows that the variation of temperature windows at different thermal levels of both systems A and B are between 15% and 30% at each gain setting, and five of them are measured to be higher and only one lower than the indicated sensitivities of S=2, S=5, and S=10. As for system D, the difference in temperature windows at gain setting from maximum to mid-point was found to be approximately 1°C. Table 9 indicates that the temperature shifts from various gain settings of both systems A and B are between 5 and 20 percent at each thermal level setting, and they are all higher than the changes of the indicated levels.

3.4 Optical Transfer Function (OTF)

The OTF describes the ability of an imaging system to reproduce the spatial frequency content of the target. In general, the image differs from the target with amplitude attenuation and phase shift. The purpose of the OTF test is to obtain a continuous curve to measure the system response as a function of spatial frequency for the imaging system based on the Fourier Transform of the line spread function (LSF). It is an objective measure of maximum resolution of a sensor in a linear operating mode at a high radiance level, which should correlate with the high frequency asymptote of the MRTD curves. Therefore, it is necessary to insure that the imaging system being tested is operating in its maximum linear region, and that the region of measurement is sufficiently isoplanatic. The LSF generated by a narrow slit can be measured by the scanning method to give its intensity distribution of the LSF of the narrow slit. The Fourier Transform of the measured LSF, which is defined as the OTF, has two terms; the modulus (amplitude) and the argument (phase). The modulation transfer function (MTF), which is the modulus of the Fourier transform, determines the amplitude response of the imaging system. In the NBS facility, a scanning slit probe is used to perform the measurement of LSF of the narrow slit target.

The OTF test setup is similar to the SiTF test (shown in figure 14) except that the positions of the coupling lens are reversed, a different target pattern (0.25 mm slit) is used, the scanning probe is replaced with a smaller scanning slit probe (0.075 mm), and a scanning motor with a control box for moving the slit probe is used. According to the size of the slit, the distance between target and sensor has to be adjusted so that the angle subtended by the slit width is much smaller (about ten times) than the instantaneous field of view (IFOV)* of the system being tested. Table 10 is a checklist for the OTF test for various imaging systems. The steps are listed below. Follow the same procedures as in the SiTF test to align the radiometric slit probe with the camera lens, to focus the slit image of the slit target, and then to position the probe horizontally until the probe's slit aperture falls in the center of the slit image of the slit target. In order to provide a high level of radiation from the source and to operate the system in the linear region, generate a modified SiTF curve at the peak of the output slit spread function for various combinations of brightness and gain controls to determine the linear region (by similar procedures as SiTF test). Afterward, adjust the blackbody source to the ΔT value found at the end of the linear region (about 20% of the ΔT which leads to curve saturation). Use the scanning motor to move the

---

* IFOV is the angle in mrad determined by dividing the size of the sensor's detector by the effective focal length of the sensor's objective lens and multiplying by 1000.

slit probe from one end of the image to the other by controlling the probe's positions from the control box. Record the output signal from the digital radiometer at each position of the slit probe as these values represent the measured LSF. The MTF can be obtained by taking the Fourier transform of the LSF.

The LSF was measured for systems A and B. After the modified SiTF was generated to locate the linear operational region for the slit image and the slit probe, the differential temperature (ΔT) for systems A and B was determined to be 18°C and 15°C respectively. By using these ΔT's, the LSF could be generated from the relative brightness of the radiometer (at such ΔT) as a function of slit probe's position while the probe is moving from one end of the image to the other. The LSFs of both systems are shown in figures 16a and 16b. The measured LSF was originally in millimeters from the position of the slit probe. It should be calibrated to milliradians in object space for output image of the infrared devices. The calibration is based on the magnification factor of the imaging equipment and the focal lengths of the coupling lens which can be established from the on-axis magnification test described in the next section.

The LSF shown in figures 16a and 16b can be analyzed by estimating the width of the function at its half amplitude points. The inverse of this value is a good indication of maximum resolution of an imaging system operating in its linear range, which corresponds to the vertical asymptote of the MRTD curves. The spreads at half amplitude points of systems A and B are found to be 5.8 mrad and 6.65 mrad, respectively. Accordingly, the maximum resolutions of these two systems are calculated to be 0.17 and 0.15 cy/mrad, which agree with the MRTD curves in figure 8.

The MTF of the imaging system is determined by using the algorithm of Fast Fourier Transform [10] and numerical analysis in order to locate the modulations other than the harmonics and to check the modulations at harmonics by both methods. The results for both systems are in agreement and are presented in figures 17a and 17b. As illustrated in figures 17a and 17b, the spatial frequency range at which the modulation reaches 0.05 to 0.02 is between approximately 0.15 and 0.2 cy/mrad, which agrees with the maximum resolution of these systems. By using the instantaneous fields of view (IFOV) given by the manufacturer (IFOV = 3.5 mrad), the nominal mid-frequency f_o (which is defined as 1/2(IFOV)) of systems A and B is equal to 0.14 cy/mrad. However, the MRTD curves of these two systems (A and B) indicated that they are approaching the asymptote at this spatial frequency (f = 0.14 cy/mrad) and the nominal mid-frequency range should be between 0.1 and 0.12 cy/mrad. In this case, the IFOV of these systems are in the range of 4 to 5 mrad, and the modulation of systems A and B are in the range of 0.2, indicating they are well-designed systems.

3.5 Geometric Transfer Characteristics

This test is to measure the on-axis magnification of the infrared imaging devices across the horizontal FOV in order to calibrate the horizontal axis in milliradians in object space. The laboratory setup is similar to the OTF test except the object is bar pattern #2 or #3 instead of a slit. The input object's subtended angle in milliradians can be calculated by the known dimensions of the bar pattern and the distance between the target and the sensor. The output image size in milliradians can be measured by scanning the slit probe to obtain the distance between a peak and a valley of the scanned bar pattern image, which represents the length of a half cycle. The output from the digital radiometer is converted to the size on the monitor by multiplying the output data with the ratio of focal lengths of the coupling lens. The on-axis magnification of the imaging system is then given as the ratio of the output image to the input object space size, either in mm/mrad or mrad/mrad, depending on the individual system.

The calculation of the magnification factor of an imaging system should use the following steps: Let the half-cycle input size in object space be W_1 mrad, and the measured distance between a peak to a valley from the radiometer be W_3 mm. The distance from the peak to the valley of the image on the monitor W_2 in mm is calculated as

$$W_2 = W_3 \cdot (f_1/f_2) \tag{2}$$

where f_1 and f_2 are the focal lengths of the coupling lens with lens #1 backing to the monitor and lens #2 backing to the slit probe. Therefore, the magnification for the imaging equipment is given as

$$M = (W_2/W_1) \qquad \text{mm/mrad} \tag{3}$$

and the magnification for the sensor and lens is given as

$$M_1 = (W_3/W_1) \qquad \text{mm/mrad} \tag{4}$$

Both patterns #2 and #3 were employed to test for on-axis magnification of systems A and B. The average values obtained from both patterns are used to calibrate the horizontal axis for the LSF. Table 11 gives the measurements and results from the magnification test.

3.6 Display Uniformity

The purpose of this test is to measure the large and small scale variations in brightness across the display when the imaging devices are viewing an object/scene of uniform temperature. This measurement is the primary interest for building diagnostics. The setup for this test is similar to the SiTF test except that the entrance aperture of the sensor under test is covered with a heavy black cloth to provide uniform input for the sensor. The output can be measured by scanning the radiometer probe across various regions of the display, manually or with a motor drive.

In the laboratory setup, the Uniformity Test was run on systems A and B, for horizontal displays only with results shown in table 12. As shown in table 12, the average standard deviation of the mean is 5.4% and 5.7% of the average output for systems A and B, respectively. The uniformity display of these two sytems is considered to be good, since their large scale variations across the horizontal display are less than 6% of the average signal output at maximum gain, (S=2).

4. CONCLUSIONS

Five infrared imaging systems (A, B, C, D, and E) were tested to evaluate their performance for building diagnostics, of which two systems (A and B) have complete sets of test results.

The MRTD test indicates that all sensors are spatial-frequency dependent as well as temperature dependent and the instrument sensitivities of systems A and B are in agreement with ASHRAE's calculations, while that of system C is not. The absolute temperature measurement reveals that data of system A is not temperature dependent, in agreement with the manufacturer's curve, while data of both systems B and C exhibit temperature dependencies, and temperature shifts from the manufacturer's curve for system B at room temperature (no curves available from the manufacturer of system C). The differential temperature measurement shows that thermal levels of systems A, B, and C respond linearly to temperature differences between target and background.

Measurements from SiTF depict that system A has smaller temperature windows than system B at identical sensitivity settings; while system B has less temperature shifts than system A at equivalent changes in thermal levels. Tests from OTF indicate almost identical MTFs are obtained for both systems A and B. The maximum resolution of these two systems are in agreement with results from the MRTD test. However, the estimated IFOV from MTF has a discrepancy from values given by the manufacturers.

Results from on-axis magnification tests are used for calibration of the horizontal axis for the OTF test. Data from the uniformity test suggest that both systems A and B have fairly uniform horizontal displays.

The results from the above laboratory evaluation give general characteristics of each of the imaging systems under test. Due to the unavailabilities and time constraints of several sensing systems, complete test results for all systems except A and B are not available. It is intended to investigate the performance of other systems at a later time, and such investigations may also include quantitative measurements other than those reported here.

5. ACKNOWLEDGEMENTS

This work was supported by the Department of Energy through an interagency agreement with the National Bureau of Standards, Interagency Agreement No. DEAI 01-76 PRO 6010, Task #008, Modification 38.

The authors would like to acknowledge the technical contributions of Douglas Pruitt and the effort of Phillip Engers and Patrick Lane. Both are cooperative education students who assisted in laboratory tests.

6. REFERENCES

[1] Wood, J.T., Cuttica, J.J. and Snow, F.J., "Application of Imaging Evaluation Technology Sensors to Heat Loss Diagnostic Sensors", Modern Utilization of Infrared Technology V, Proc. SPIE Vol. 197, pp. 108-114, Bellingham, WA, 1979.

[2] Kaplan, H., "An Update of Commercial Infrared Sensing and Imaging Instruments", An International Conference on Thermal Infrared Sensing for Diagnostics and Control (Thermosense VI) Proc. SPIE Vol. 446, pp.239-246, Bellingham, WA, 1983.

[3] McIntosh, G.B. and Filippene, A.F., "Minimum Resolvable Temperature Difference (MRTD) Testing: Equipment Specification for Building Performance Diagnostics", Thermal Infrared Sensing Applied to Energy Conservation in Building Envelopes (Thermosense IV), Proc. SPIE Vol. 313, pp 102-111, Bellingham, WA, 1981.

[4] Wood, J.T. and Grot, R.A., "Description of a Facility for Evaluating Infrared Imaging Systems for Building Applications", Thermal Infrared Sensing Diagnostics (Thermosense V), Proc. SPIE Vol. 371, pp. 146-149, Bellingham, WA, 1982.

[5] Burrer, G.J., "Update on Proposed ASHRAE Standard on Requirements for Infrared Surveys", Thermal Infrared Sensing Applied to Energy Conservation in Building Envelopes (Thermosense III), Proc. SPIE Vol. 254, pp. 148-153, Bellingham, WA, 1980.

[6] Snow, F.J., "American Society of Heating, Refrigeration, and Air Conditioning Engineers (ASHRAE) Thermographic Standard 101P", Thermal Infrared Sensing Applied to Energy Conservation in Building Envelopes (Thermosense IV), Proc. SPIE Vol. 313, pp. 94-98, Bellingham, WA, 1981.

[7] ASHRAE Standard 101-83, Application of Infrared Sensing Devices to the Assessment of Building Heat Loss Characteristics, ASHRAE, Atlanta, GA, 1983.

[8] Wood, J.T., "Evolving American Society for Testing and Materials (ASTM) Procedures on Use of Infrared (IR) Imaging Devices for Building Diagnostics", Thermal Infrared Sensing Applied to Energy Conservation in Building Envelopes (Thermosense III), Proc. SPIE Vol. 254, pp. 154-158, Bellingham, WA, 1980.

[9] Kantsios, A.G., "Progress on American Society for Testing and Materials (ASTM) Practice on Thermographic Inspections of Wood Frame Buildings", Thermal Infrared Sensing Applied to Energy Conservation in Building Envelopes (Thermosense IV), Proc. SPIE Vol. 313, pp. 99-101, Bellingham, WA, 1981.

[10] Ahmed, N. and Rao, K.R., Orthogonal Transforms for Digital Signal Processing. Berlin - Heidelberg: Springer-Verlag, 1975, ch. 4, p. 79.

Table 1. Specifications of Building Diagnostic Sensors

	IR System					
DATA DESCRIPTION	A B (Dual Channel)	C	D	E	F	G
Field of View	w/33mm lens 20°x20° NFOV 40°x40° WFOV	14°x18°	7.5°x18°	6°x12°	w/50mm lens 20°x20° NFOV 40°x40° WFOV	w/2.5X afocal 6.8°x11.2° NFOV 19°x28° WFOV
Instantaneous Field of View	3.5 mrad NFOV 7.0 mrad WFOV	2.0 mrad	2.2 mrad	2.0 mrad	2.4 mrad NFOV 4.8 mrad WFOV	0.73 mrad NFOV 1.8 mrad WFOV
F#	1.8	-	1.5	1.0	-	1.0
EFL	1.3" NFOV 0.7" WFOV	-	1.5"	2.5"	-	2.75" NFOV 1.1" WFOV
Additional Optics	52mm 99mm 191mm	3X afocal 10X afocal	None	None	100mm 75mm	5X afocal
Display	AGA CRT (5" diag)	525 line CRT	Monocular Eyepiece (LED)	Monocular Eyepiece (CRT)	525 line CRT	525 line CRT
Detector Type and Number	1 InSb (3-5.6) 1 HgCdTe (8-14)	HgCdTe	6 InSb	48 PbSe	DTGFB(PEV)	2 HgCdTe
Spectral Range	3-5.6 microns 8-14 microns	8-12 microns	3-5.4 microns	3-5 microns	8-12 microns	8-12 microns
Interlace	4:1	2:1	10:1	1:1	-	2:1
Quoted Sensitivity	0.1°C @ 30°C 100 Pixels/line	0.1°C MDT @ 30°C 150 pixes/line	0.1° NET (peak-to-rms)	0.2°C (peak)	0.2°C NET @ 8LP/mm	0.2°C NET 0.4°C MRT @ 0.27 c/mr
Size and Weight	Scanner:w/o lens 7 lbs. 9.3"x10.2"x6.5"	24 lbs. Scanner:4 lbs. 6.1"x4.3"x4.8"	(w/battery) 7.5 lbs. 10"x9"x6"	6.6 lbs. 9.4"x5.5"x3.3" (w/o battery)	Camera:w/o lens 24 lbs. 10"x8"x8"	24 lbs (total) Scanner:11 lbs. 10.7"x7.3"x9.1"
Power Requirements	100, 120, 220, 240 VAC 8-15 VDC	12 VDC or 110 VAC	1.5 W Battery Charger: 117 VAC	6 VDC 110/220 VAC	115 VAC	12 VDC 110 VAC
Operating Temperatue Range	-15°C/+55°C	-	-	-20°C/+55°C	-32°C/+49°C	-15°C/+55°C
Cooling	Cryogenic (liquid nitrogen)	Cryogenic (liquid nitrogen)	J-T Cryostat	Split Sterling	None	J-T Cryostat
Minimum Focus	20 cm (WFOV)	13 cm	200 cm	100 cm	244 cm	150 cm

NFOV : Normal Field of View
WFOV : Wide Field of View
F# : Aperture
EFL : Effective Focal Length

Conversion Factors for SI Units : 1 lb = 0.4536 kg
1 in = 2.54 cm

Table 2. Instrument Items for the Evaluation Facility

Item	Status
1. Target Source Table	Constructed
2. Vertical Motion Jactuator	Purchased
3. Target Source Mounting Plate	Constructed
4. Source Mounting Block (Wood)	Constructed
5. Blackbody Source	Purchased
6. Blackbody Source Controller	Purchased
7. Background Plate	Constructed
8. Target Pattern Holder	Constructed
9. Sensor/Monitor Table	Constructed
10. Sensor/Monitor Rotating Table	Purchased
11. Sensor/Monitor Mounting Plate	Constructed
12. Sensor Mounting Block	Constructed
13. Coupling Lens (2)	Purchased
14. Optical Rail (Modified)	Available in-house
15. Radiometric Eyepiece	Purchased
16. Fiber Optic Cable	Purchased
17. Photomultiplier Tube	Purchased
18. PMT Power Supply/Signal Monitor	Purchased
19. Motor Control Scanner	Purchased
20. Casters	Purchased
21. Display Mounting Block (Wood)	Constructed
22. Display Rotating Table	Available in-house
23. Display Mounting Plate	Constructed
24. Refrigerator System for Chamber	Available in-house
25. Computer Facility (Future Items)	Available in-house

Table 3. Test Target Sizes Required for Building Diagnostic Sensors

SYSTEM	FOV	Min. Wall Width (cm)	Dist. From Wall (cm)	Min. Focus Dist. (cm)	IFOV (mrad)	Target Pattern Size at Limiting Distance (cycles/centimeter) $f_o/4$	$f_o/2$	$5f_o/6$	f_o	$5f_o/4$	$3f_o/2$	ASHRAE Class A /ASTM	ASHRAE Class B
A and B	20^ox20^o	80	227	50	3.5	.157	.315	.524	.629	.787	.944	.52	.13
C	14^ox18^o	80	253	13	2.0	.247	.494	.823	.988	1.235	1.482	.52	.13
D	7.5^ox18^o	144	455	200	2.2	.125	.250	.416	.500	.624	.749	.52	.13
E	6^ox12^o	120	571	100	2.0	.109	.219	.365	.438	.547	.657	.52	.13
F	20^ox20^o	80	227	244	2.4	.213	.427	.712	.854	1.067	1.281	.52	.13
G	19^ox28^o	88	177	150	1.8	.392	.785	1.308	1.569	1.962	2.354	.52	.13

Table 4. Parameters Evaluated for Each Infrared System

Parameter Evaluated	IR System				
	A	B	C	D	E
Minimum Resolvable Temperature Difference (MRTD)	X	X	X	X	X
Temperature Calibration	X	X	X		
Signal Transfer Function (SiTF)	X	X		X	
Optical Transfer Function (OTF)	X	X			
Geometric Transfer Function (GTF)	X	X			
Display Uniformity	X	X			

Table 5. Checklist for MRTD Testing of Sensors

Facility Component . Number	IR System					
	A B	C	D	E	F	G
1 - 6	X	X	X	X	X	X
7*	X Use H Marks	X Use H Marks	X Use V Marks	X Use V Marks	X Use H Marks	X Use V Marks
8	X w/Patterns #1 - #5	X w/Patterns #1 - #5 Repeat #3 - #5	X w/Patterns #1 - #5	X w/Patterns #1 - #5	X w/Patterns #1 - #5 Repeat #3 - #5	X w/Patterns #1 - #5 Repeat #2 - #5
9 - 12	X	X	X	X	X	X
Estimated Distance From Tgt to Sensor	45.4" or 115 cm	50.5" or 128 cm Retest at 101" or 256 cm	91.5" or 232 cm	114.5" or 291 cm	45.4" or 115 cm Retest at 90.8" or 230 cm	35.9" or 91 cm Retest at 107.7" or 274 cm
Focus Pattern	#5	#5	#5	#4	#5	#5

* "Use H Marks" means to use the marks which mark the horizontal Field of View limits on the Background Plate (See Insert in Figure 1) when setting the distance between the Target Pattern and the Sensor under test.

Mark (x) means to make sure the facility components are in place and used as indicated.

Table 6. Parameters Determined from Absolute Temperature Measurements

System	Background Temperature(°C)	Parameters		
		A*	B*	C*
A (S=2)	-20	201126	2550	1.70
	-1	290189	2716	1.31
	13	318218	2755	1.23
	24	351344	2797	1.17
	All Data	333889	2818	1.04
Given by Manufacturer		552855	2994	1.0
B (S=2)	-20	10328	1052	5.22
	1	23208	1274	5.74
	5	29549	1318	6.42
	14	26623	1306	5.99
	25	39234	1394	6.79
Given by Manufacturer	22	-3762	1510	-0.45

* A, B, and C are instrument parameters given in eq. (1).

Table 7. Checklist for SiTF Testing of Sensors

Facility Component Number	IR System A B	C	D	E	F	G
1 - 7	X	X	X	X	X	X
8	X w/Pattern #6	X w/Pattern #6	X w/Pattern #6	X w/Pattern #6	X w/Pattern #6	X w/Pattern #6
9 - 12	X	X	X	X	X	X
13	X Lens 1 100mm and Lens 2 24mm	X Lens 1 100mm and Lens 2 24mm	X 50mm	X 24mm	X Lens 1 100mm and Lens 2 24mm	X Lens 1 100mm and Lens 2 24mm
14	X	X	X	X	X	X
15	X .018" Scanning Probe	X .018" Scanning Probe	X .018" Scanning Probe	X .018" Scanning Probe	X .018" Scanning Probe	X .018" Scanning Probe
16 - 18	X	X	X	X	X	X
Distance From Tgt to Sensor	45" or 115 cm	101" or 256 cm	91.5" or 232 cm	114.5" or 291 cm	90.8" or 230 cm	107.7" or 274 cm

* "Use H Marks" means to use the marks which mark the horizontal Field of View limits on the Background Plate (See Insert in Figure 1) when setting the distance between the Target Pattern and the Sensor under test.

Mark (x) means to make sure the facility components are in place and used as indicated.

Table 8. Temperature Windows from SiTF Test

SYSTEM	THERMAL LEVEL	TEMPERATURE WINDOWS OF SENSITIVITY (GAIN) (°C)		
		S = 2	S = 5	S = 10
A	22	2.55	6.25	9.87
	26.5	2.35	5.11	8.58
	28	2.10	4.71	8.40
B	50	3.20	7.12	12.76
	54	*	6.68	11.87
	56	2.70	6.47	11.48
		Gain = MAX	Gain = 1/2(MAX)	
D	MAX	2.93	3.77	

* Missing data

Table 9. Temperature Shift from SiTF Test

SYSTEM	CHANGE IN THERMAL LEVEL	TEMPERATURE SHIFT OF SENSITIVITY (GAIN) (°C)		
		S = 2	S = 5	S = 10
A	22 - 26.5	6.0	5.9	5.5
	26.5 - 28	2.4	1.9	1.7
	22 - 28	8.4	7.8	7.2
B	50 - 54	*	4.5	4.6
	54 - 56	*	2.3	2.0
	50 - 56	7.0	6.8	6.6

* Missing data

Table 10. Checklist for OTF Testing of Sensors

Facility Component Number	IR System					
	A B	C	D	E	F	G
1 - 7	X	X	X	X	X	X
8	X w/Pattern #7	X w/Pattern #7	X w/Pattern #7	X w/Pattern #7	X w/Pattern #7	X w/Pattern #7
9 - 12	X	X	X	X	X	X
13	X Lens 1 24mm and Lens 2 100mm	X Lens 1 50mm and Lens 2 100mm	X 200mm	X 100mm	X Lens 1 100mm and Lens 2 50mm	X Lens 1 50mm and Lens 2 100mm
14	X	X	X	X	X	X
15	X .003" Scanning Slit	X .003" Scanning Slit	X .003" Scanning Slit	X .003" Scanning Slit	X .003" Scanning Slit	X .003" Scanning Slit
16 - 18	X	X	X	X	X	X
Distance From Tgt to Sensor	45" or 115 cm	101" or 256 cm	91.5" or 232 cm	114.5" or 291 cm	90.8" or 230 cm	107.7" or 274 cm

* "Use H Marks" means to use the marks which mark the horizontal Field of View limits on the Background Plate (See Insert in Figure 1) when setting the distance between the Target Pattern and the Sensor under test.

Mark (x) means to make sure the facility components are in place and used as indicated.

Table 11. Measurements and Results from On-Axis Magnification Test

		System A		System B	
		Pattern		Pattern	
		#2	#3	#2	#3
Input: Target	W_1(mrad)	8.77	5.80	8.77	5.80
Output: Slit Position	W_3(mm)	5.80	3.60	4.70	3.075
Image on Monitor	W_2(mm)	1.392	0.868	1.128	0.738
M^*	(mm/mrad)	0.16	0.15	0.13	0.13
Average M^*	(mm/mrad)	0.155		0.13	
M_1^{**}	(mm/mrad)	0.65		0.54	

* Magnification factor of IR system.
** Magnification factor of IR system and lens.

Table 12. Results from Uniformity Test

	System A		System B		
Thermal Level	26	28	54	56	58
Average Relative Brightness	31.21	30.48	31.66	31.66	31.01
Standard Deviation of the Mean	1.70	1.65	1.77	1.82	1.82
Percentage of Variation	5.40	5.40	5.60	5.75	5.88
Average Percentage of Variation	5.40			5.74	

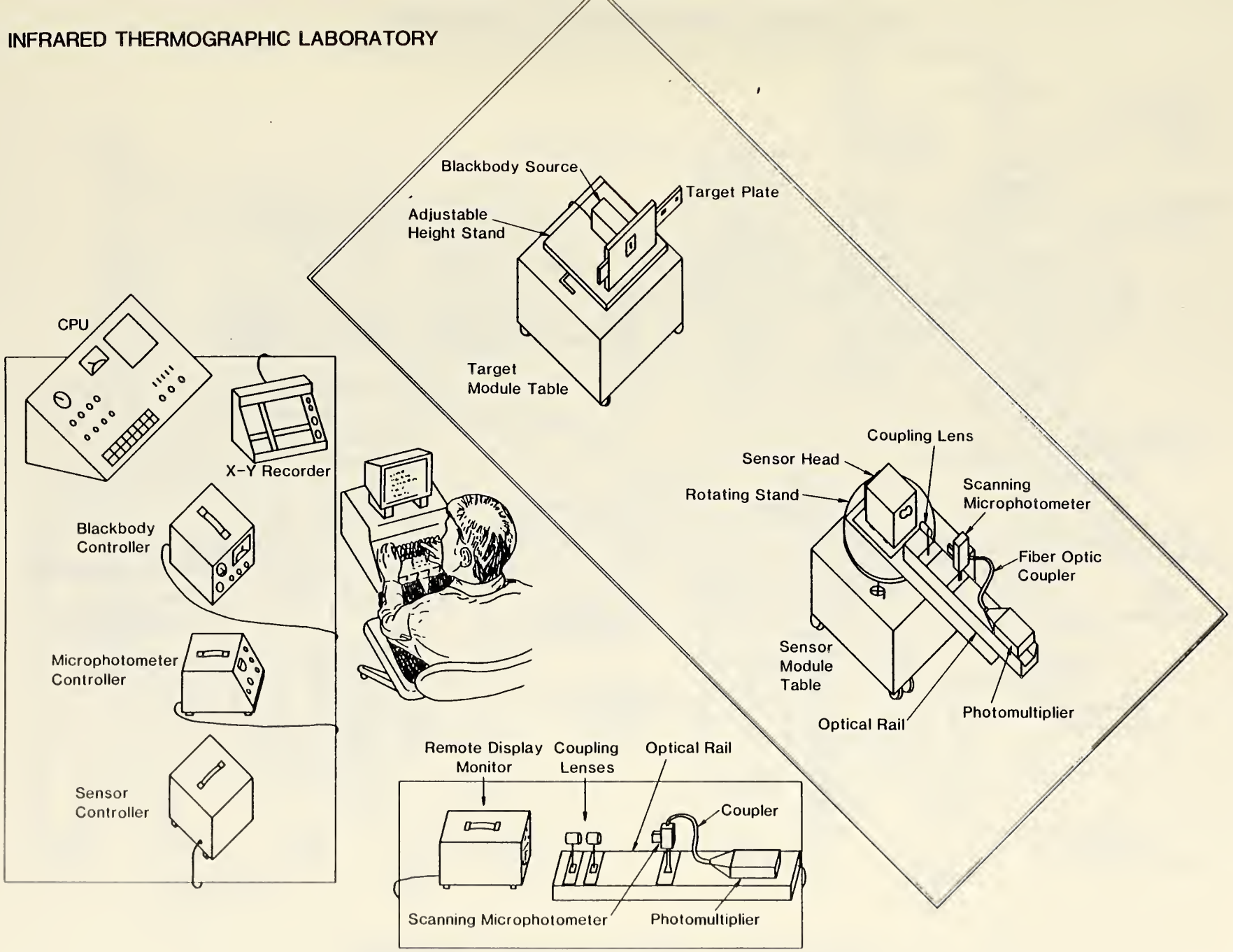

Figure 1. Overall Facility Concept

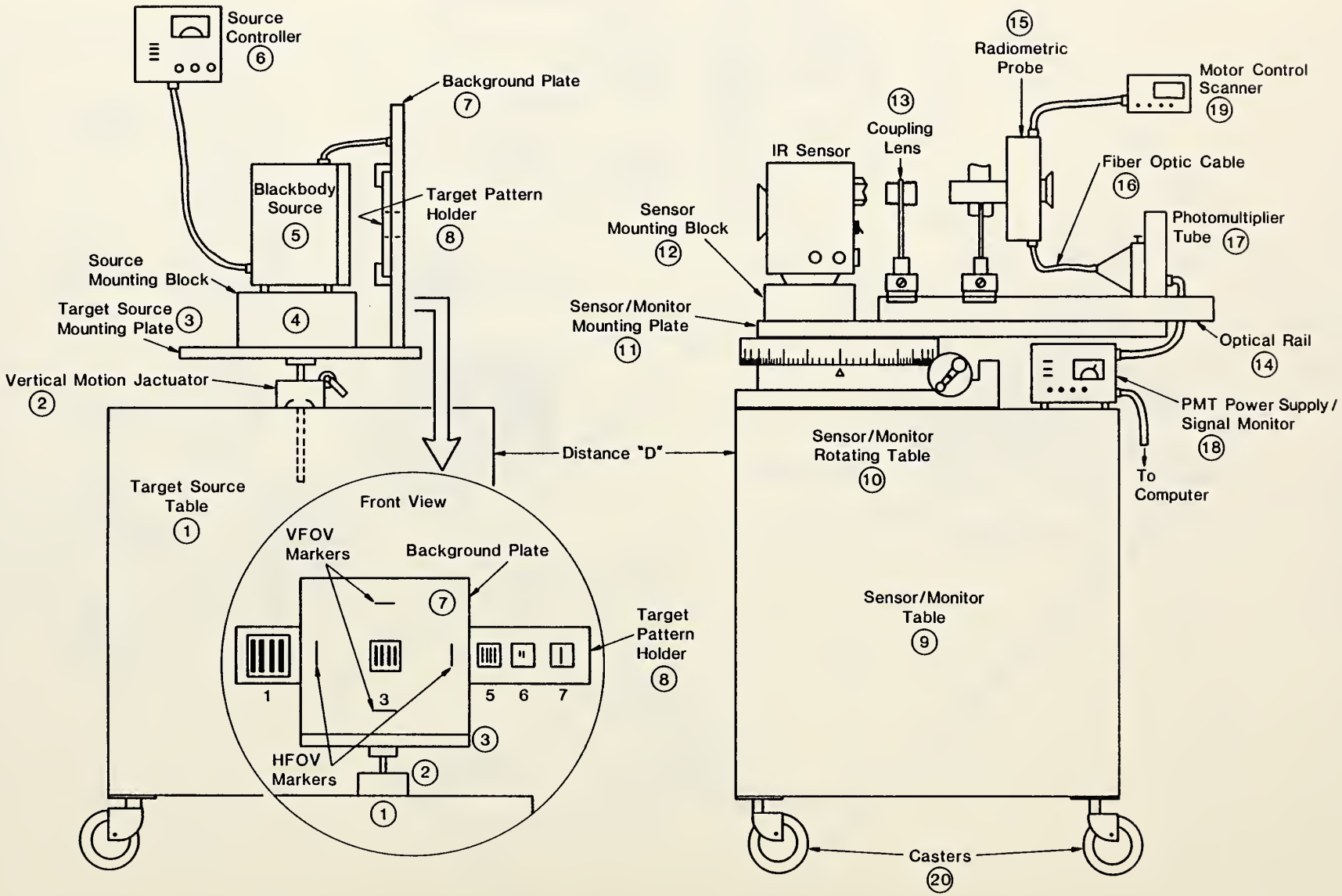

Figure 2. Basic Configuration for Test Sensor with Eyepiece

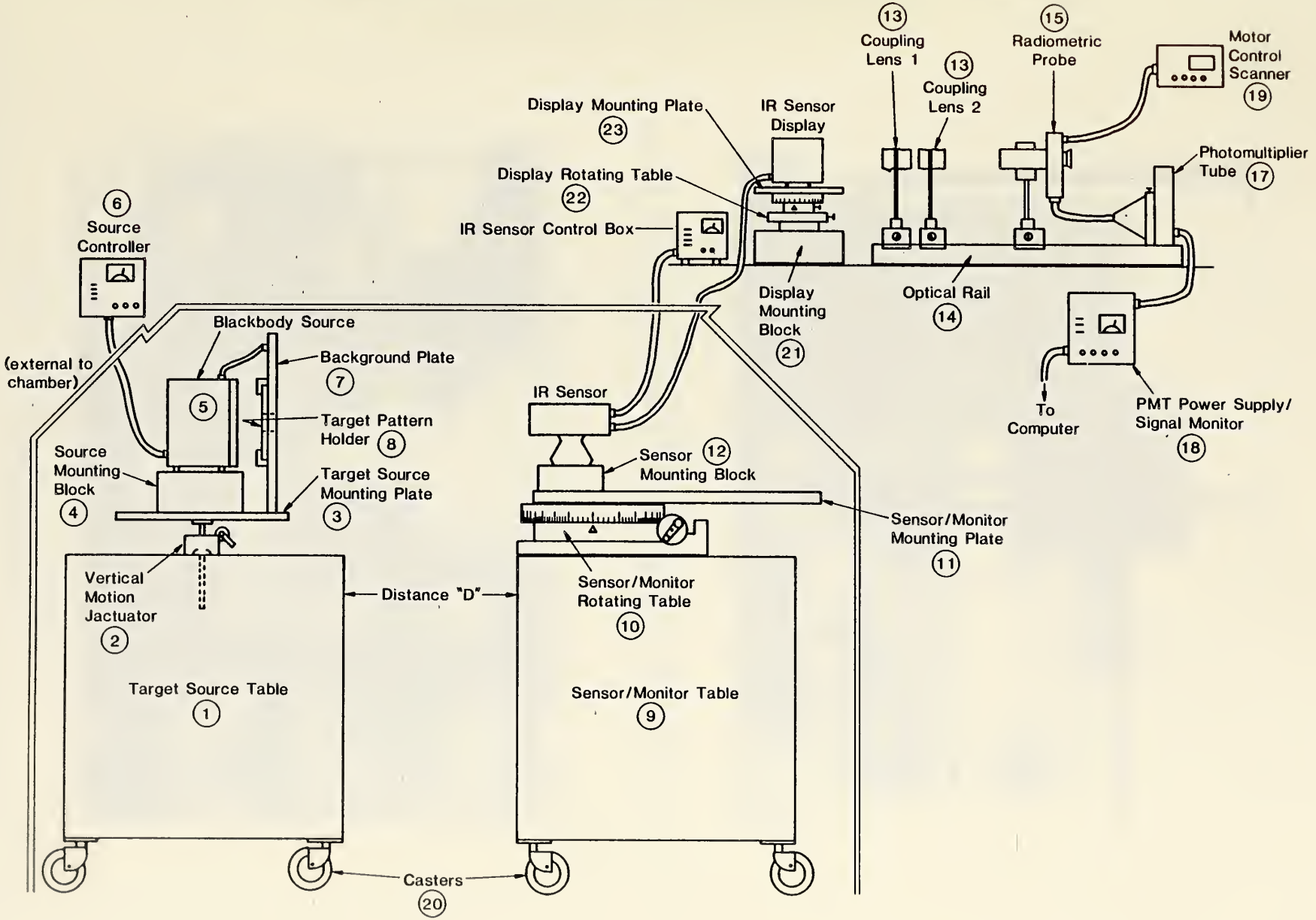

Figure 3. Basic Configuration for Test Sensor with Remote Display Monitor

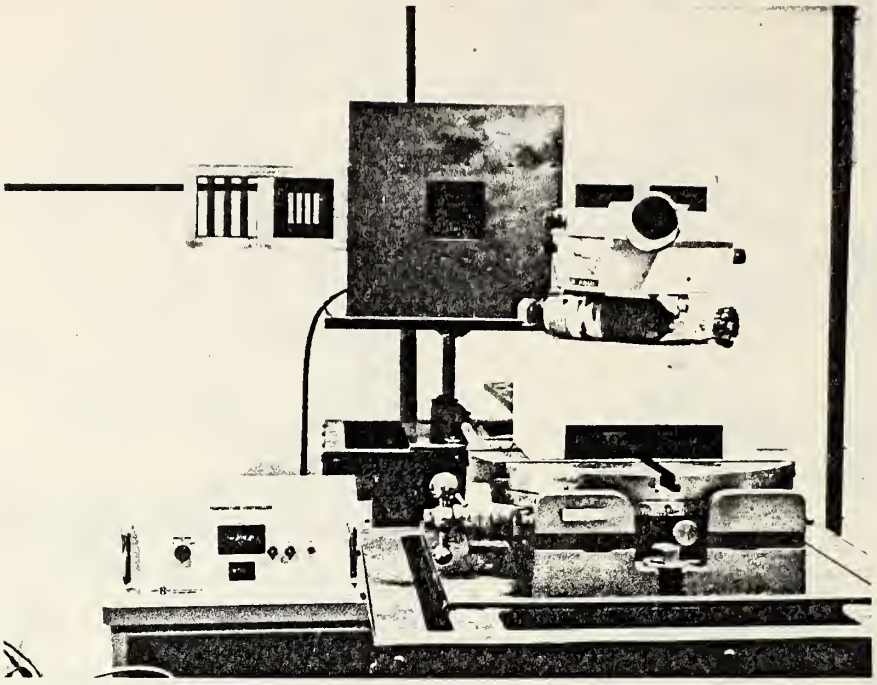

For MRTD Test

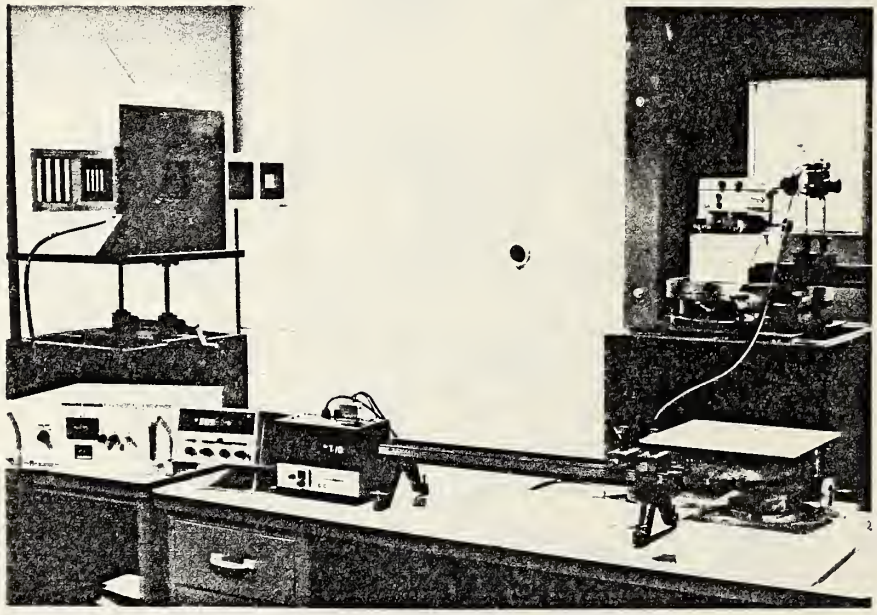

For Other Tests

Figure 4. Overall Facility Setup for Imaging Systems with Eyepiece

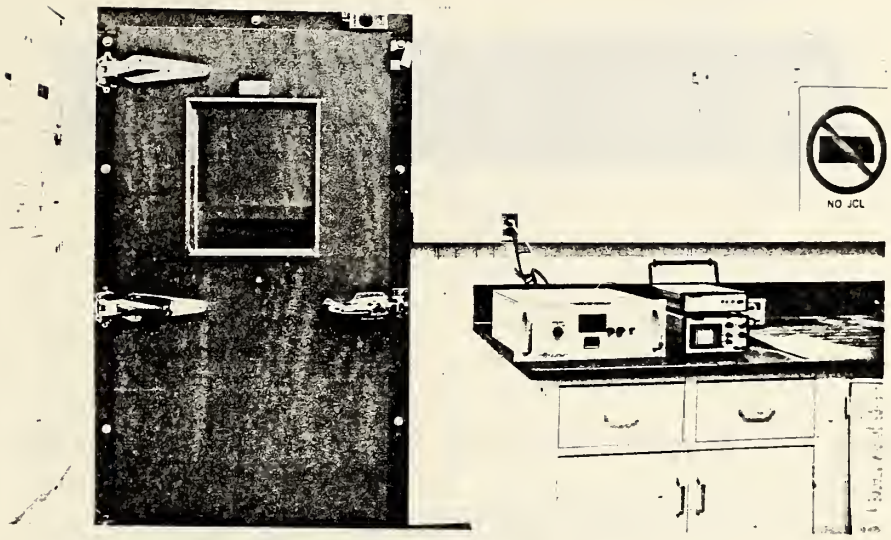

Control Room Outside Environmental Chamber

Inside Environmental Chamber

Figure 5. Overall Facility setup for Imaging Systems with Remote Display Monitor

Figure 6. Target Patterns Used for Various Tests

Figure 7. Minimum Resolvable Temperature Difference (MRTD) Test Pattern in Target Module

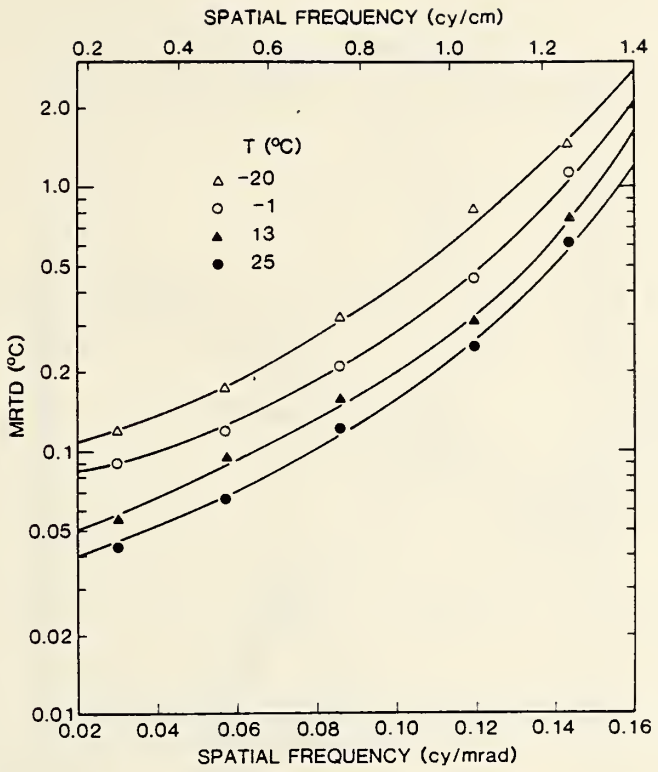

Figure 8a. Minimum Resolvable Temperature Difference (MRTD) versus Spatial Frequency at Various Background Temperatures T of System A (S=2)

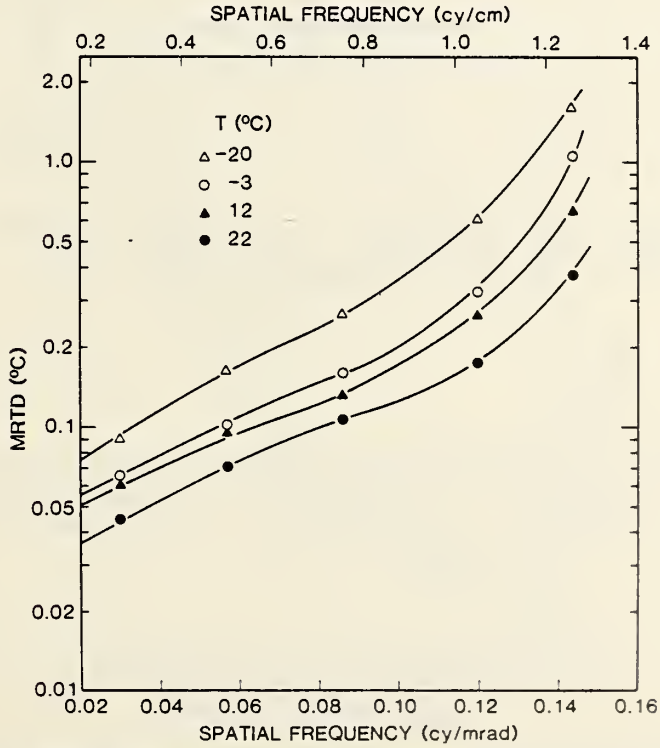

Figure 8b. Minimum Resolvable Temperature Difference (MRTD) versus Spatial Frequency at Various Background Temperatures T of System B (S=5)

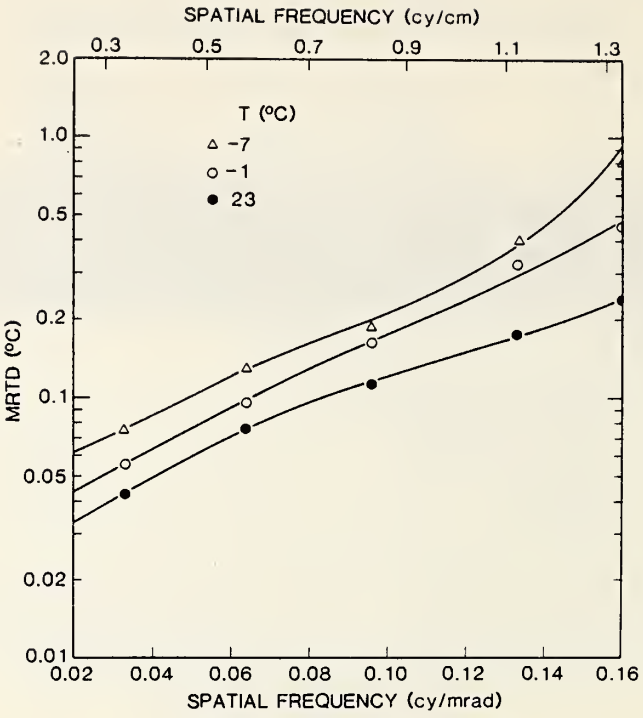

Figure 8c. Minimum Resolvable Temperature Difference (MRTD) versus Spatial Frequency at Various Background Temperatures T of System C (S=10)

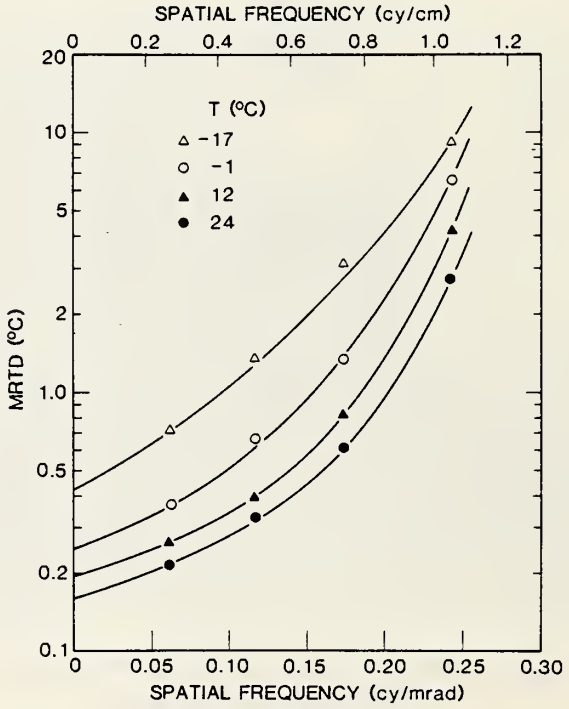

Figure 8d. Minimum Resolvable Temperature Difference (MRTD) versus Spatial Frequency at Various Background Temperatures T of System D

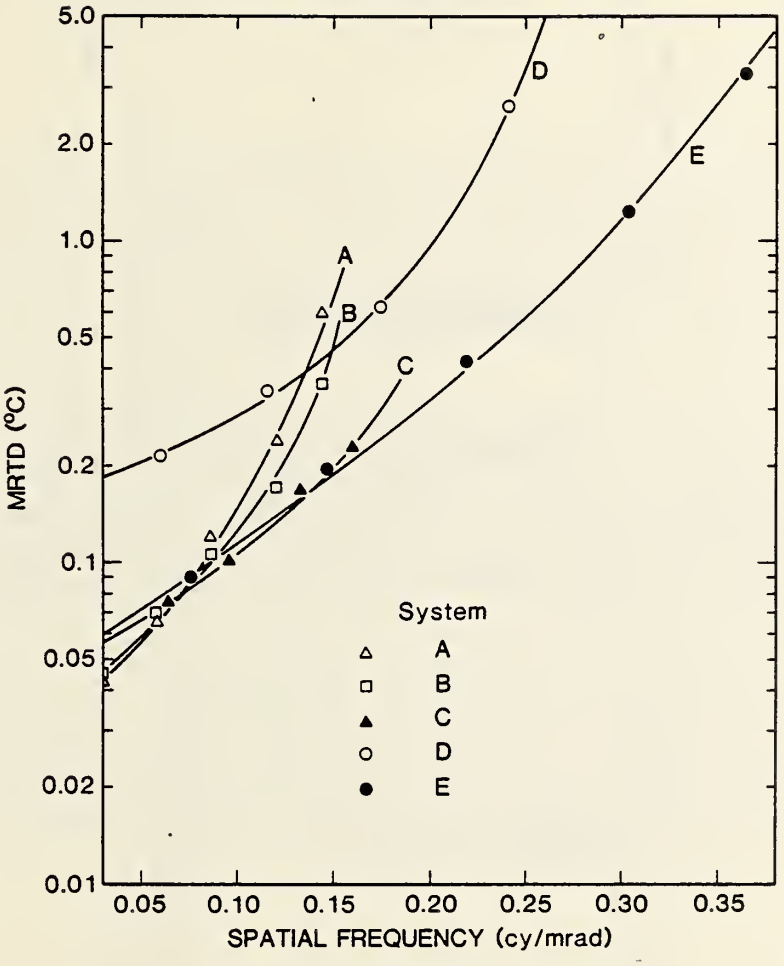

Figure 8e. Minimum Resolvable Temperature Difference (MRTD) versus Spatial Frequency of Systems A, B, C, D, and E (Blackground Temperature T $\simeq 23^{o}C$)

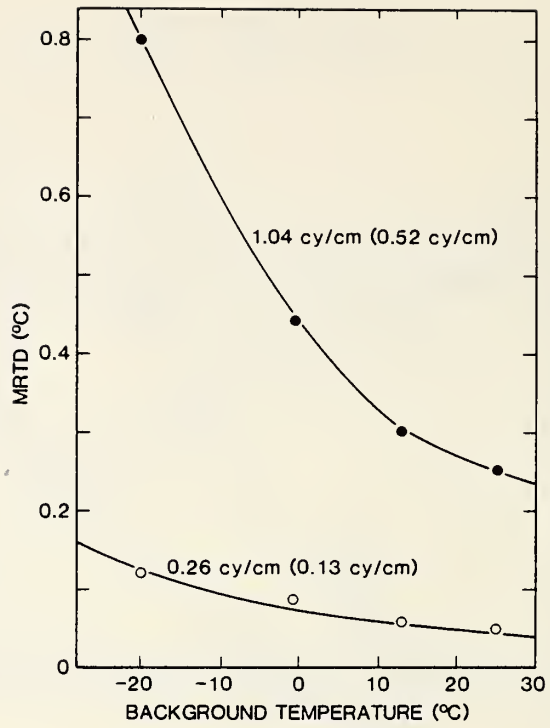

Figure 9a. Minimum Resolvable Temperature Difference (MRTD) versus Background Temperature of System A (S=2) for the Two ASHRAE Specified Test Frequencies

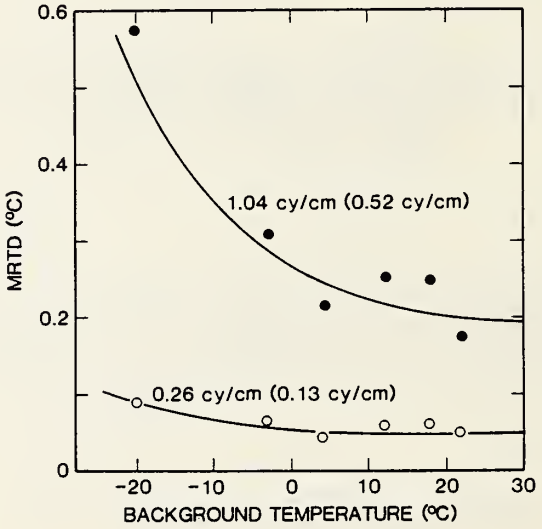

Figure 9b. Minimum Resolvable Temperature Difference (MRTD) versus Background Temperature of System B (S=5) for the Two ASHRAE Specified Test Frequencies

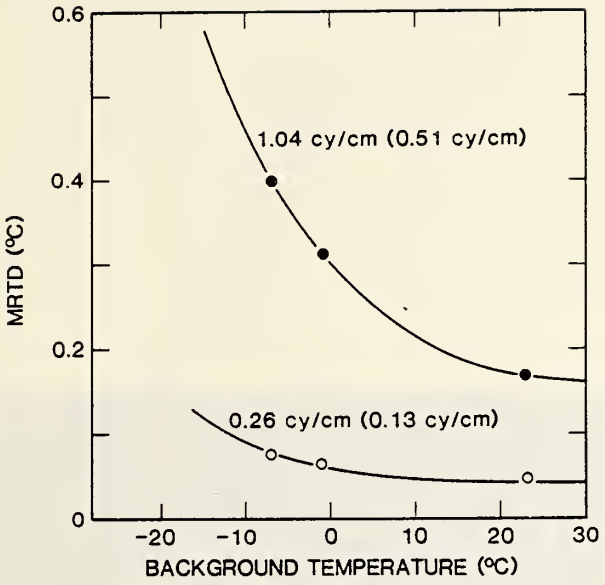

Figure 9c. Minimum Resolvable Temperature Difference (MRTD) versus Background Temperature of System C (S=10) for the Two ASHRAE Specified Test Frequencies

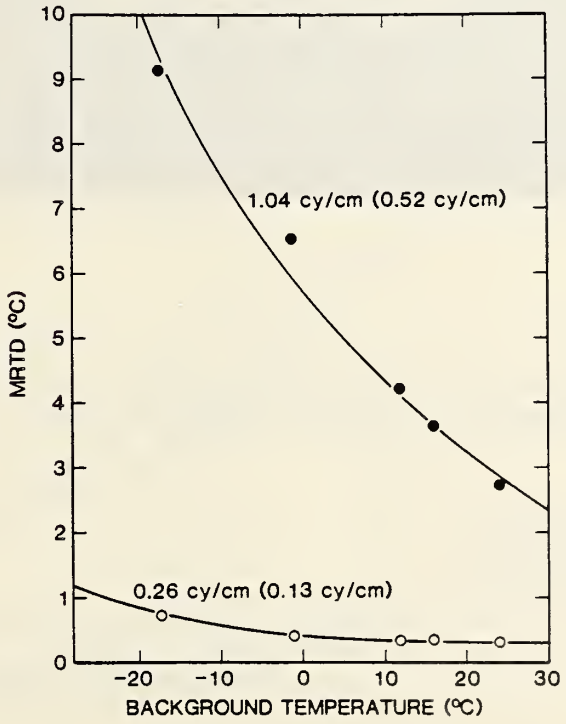

Figure 9d. Minimum Resolvable Temperature Difference (MRTD) versus Background Temperature of System D for the Two ASHRAE Specified Test Frequencies

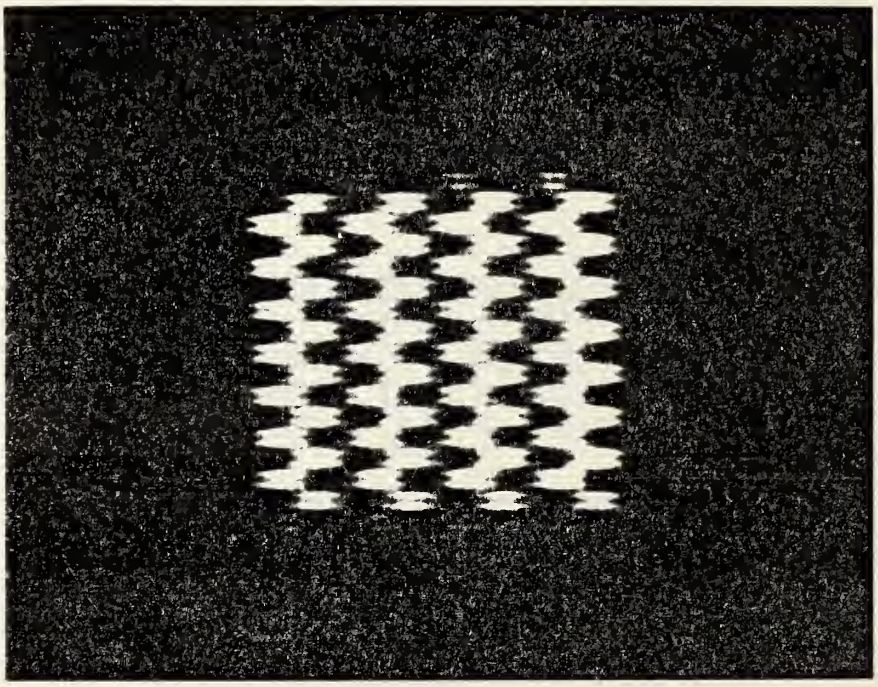

Figure 10. Image Display of System C for Pattern #4 at Background Temperature of -17°C

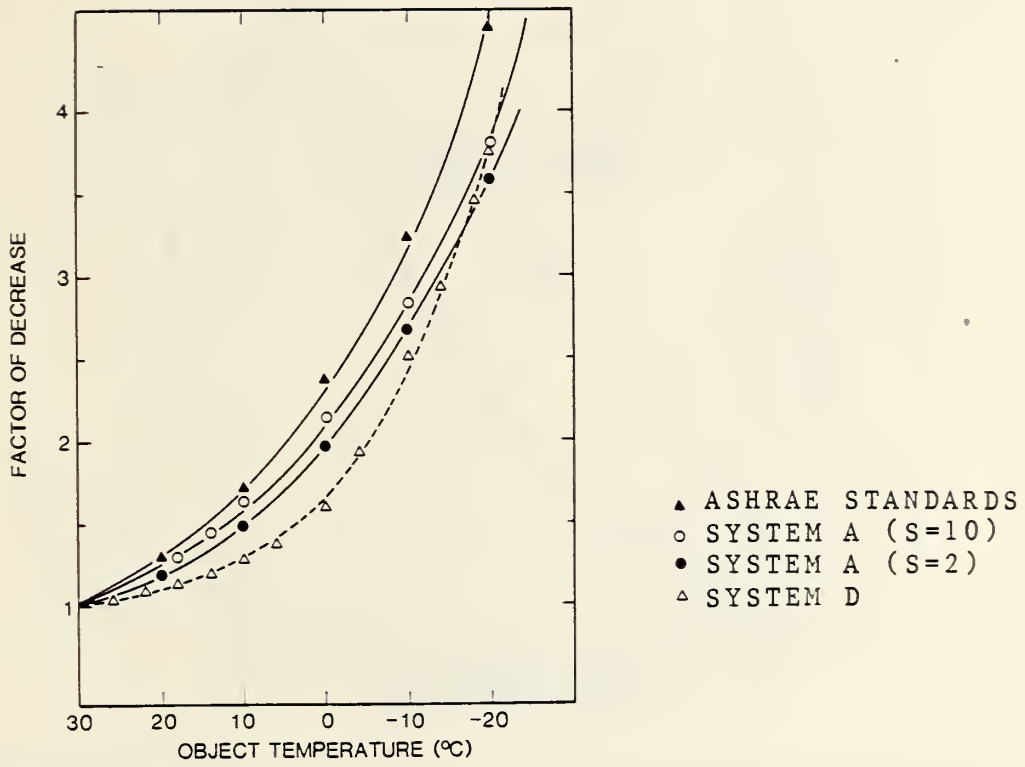

Figure 11a. Factor of Decrease for the Instrument Sensitivity Versus Object Temperature of Systems A and D (Using 30°C as Reference)

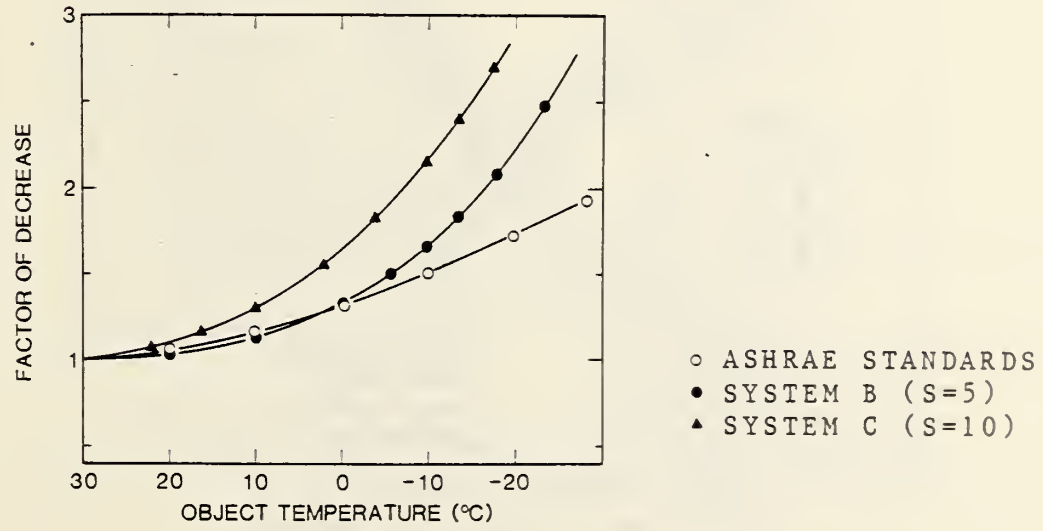

Figure 11b. Factor of Decrease for the Instrument Sensitivity Versus Object Temperature of Systems B and C (Using 30°C as Reference)

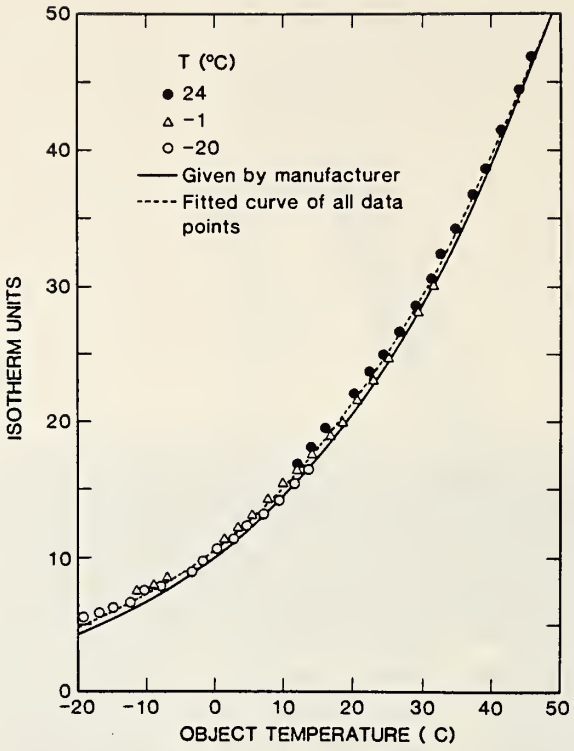

Figure 12a. Absolute Temperature Calibration Curves of System A at Various Background Temperatures T (S=2, Aperture = f/1.8)

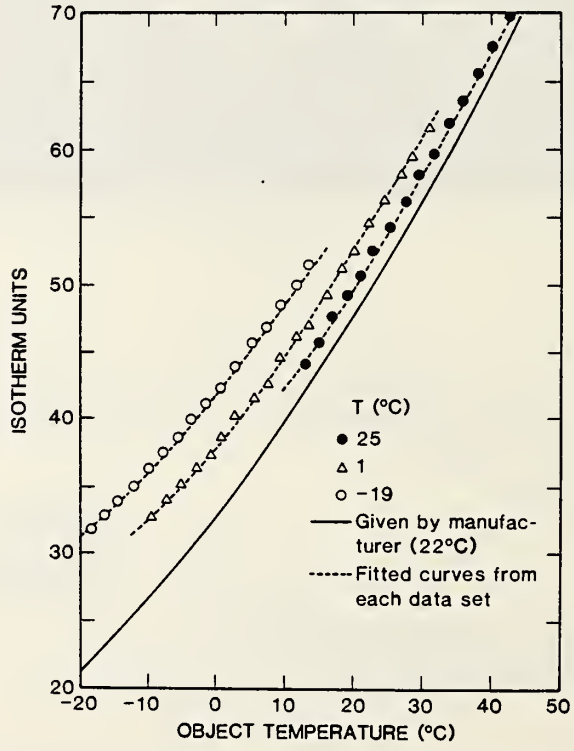

Figure 12b. Absolute Temperature Calibration Curves of System B at Various Background Temperatures T (S=2, Aperture = f/1.8)

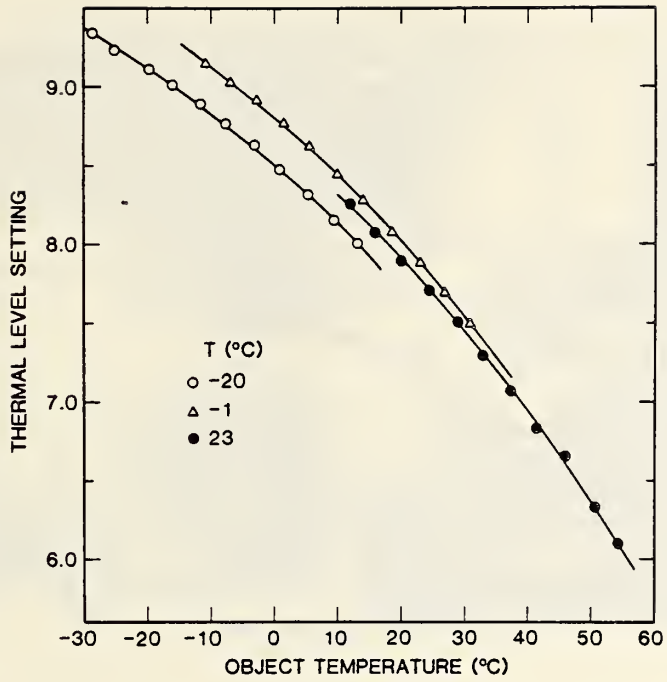

Figure 12c. Absolute Temperature Calibration Curves of System C at Various Background Temperatures T (S=10)

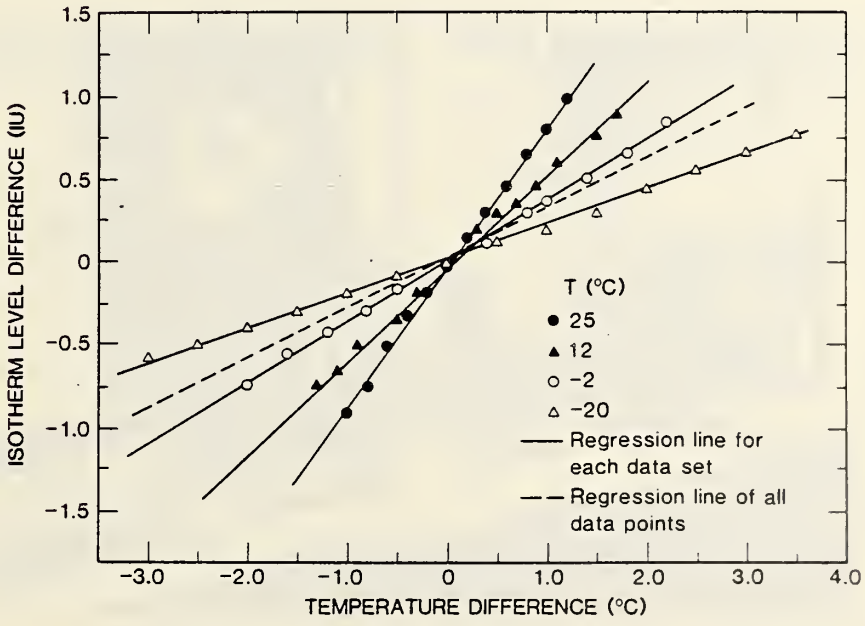

Figure 13a. Differential Temperature Calibration Curves of System A at Various Background Temperatures T (S=2)

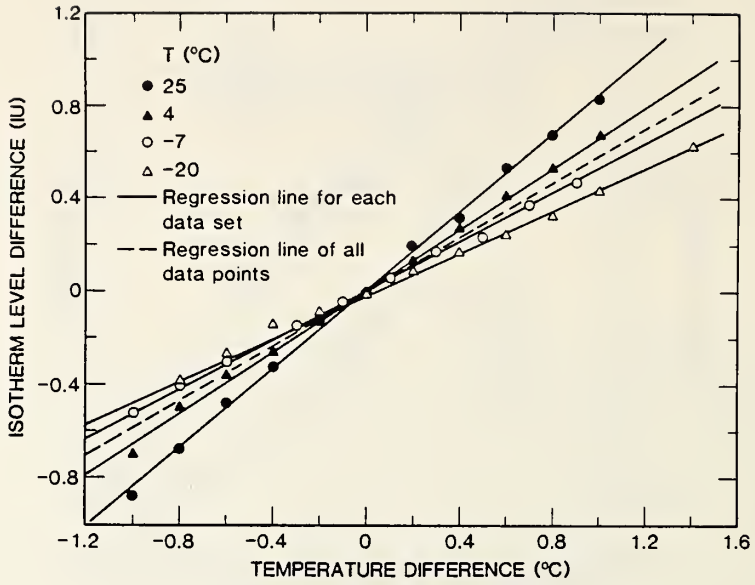

Figure 13b. Differential Temperature Calibration Curves of System B at Various Background Temperatures T (S=2)

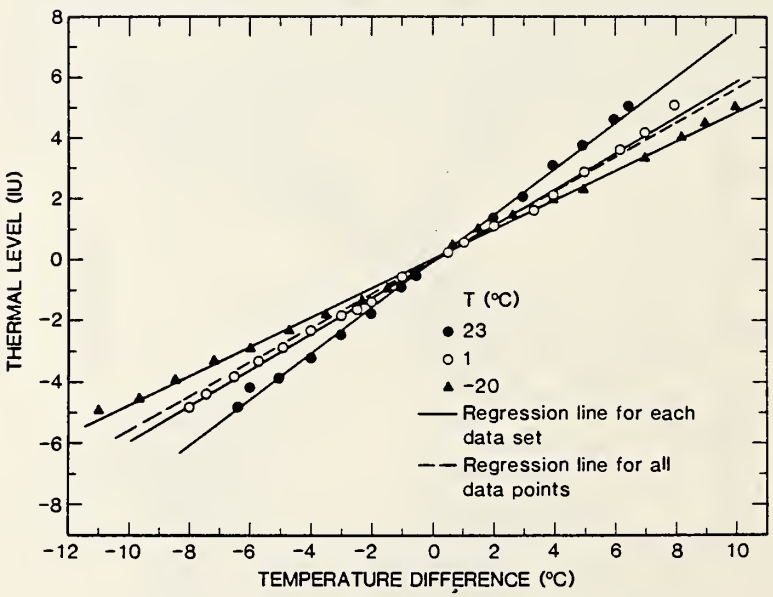

Figure 13c. Differential Temperature Calibration Curves of System C at Various Background Temperatures T (S=10)

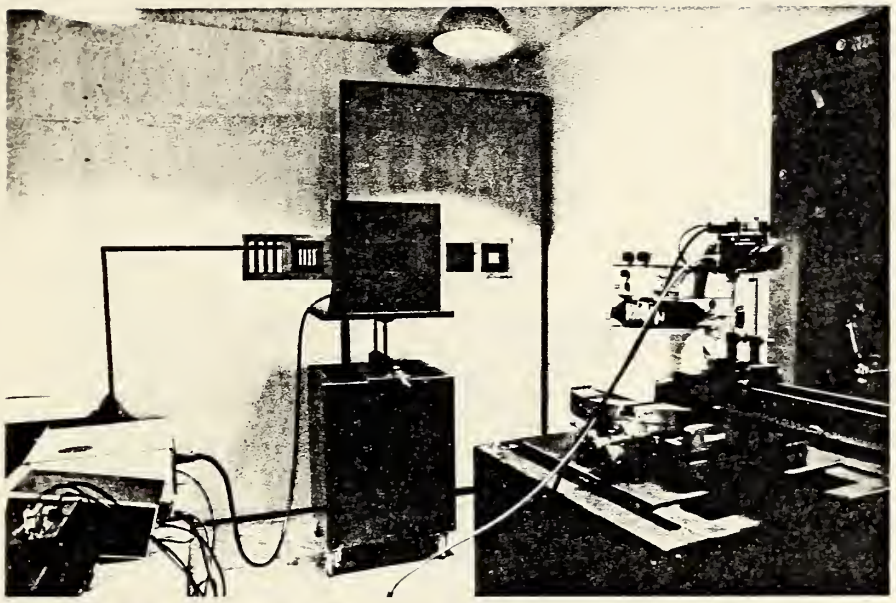

System with Eyepiece Display

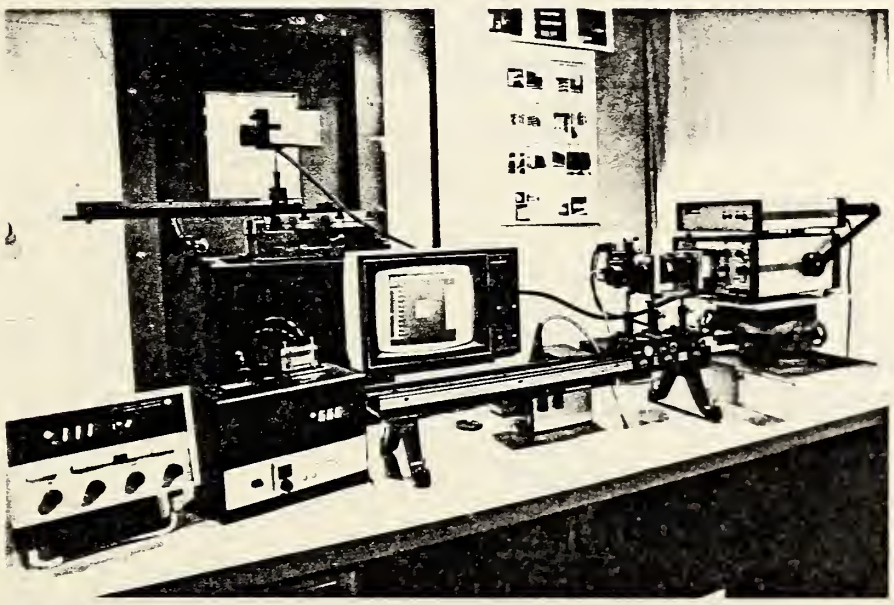

System with Remote Monitor Display

Figure 14. Instrumentation Setup for Signal Transfer Function (SiTF) Tests

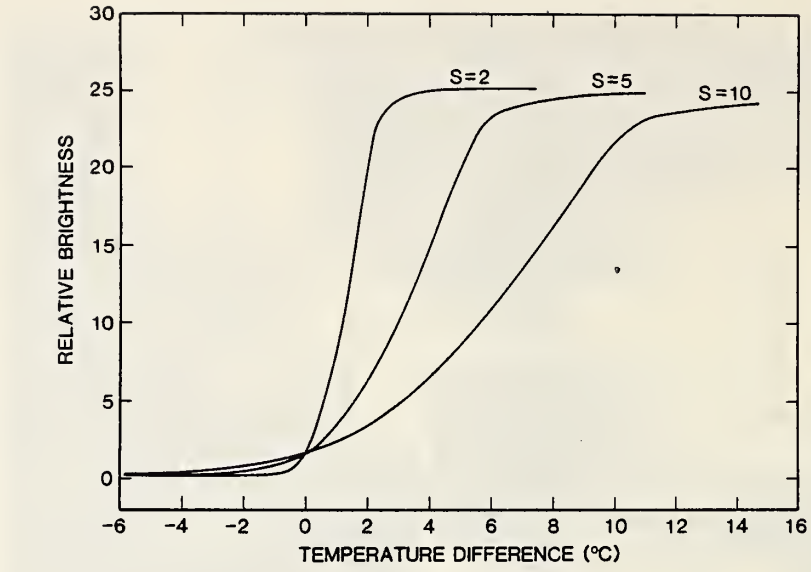

Figure 15a. Relative Brightness versus Temperature Difference from SiTF Test of System A at Constant Thermal Level (TL=26.5) for Various Gains

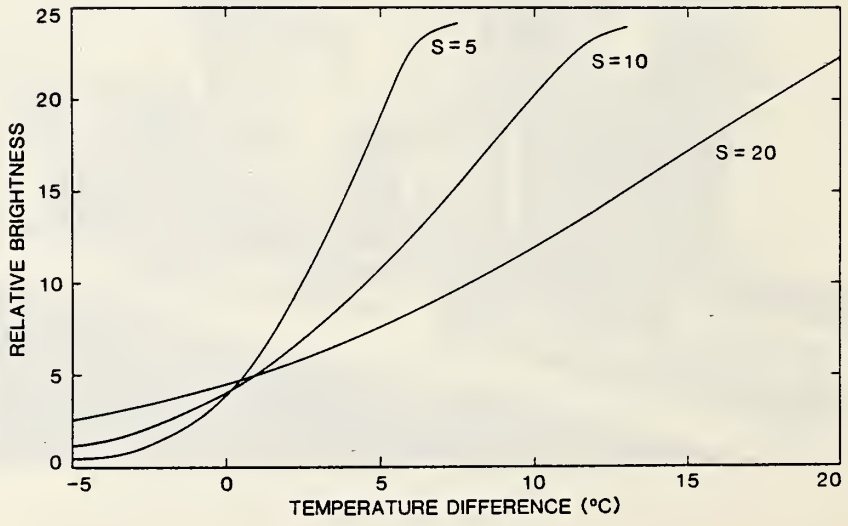

Figure 15b. Relative Brightness versus Temperature Difference from SiTF Test of System B at Constant Thermal Level (TL=54) for Various Gains

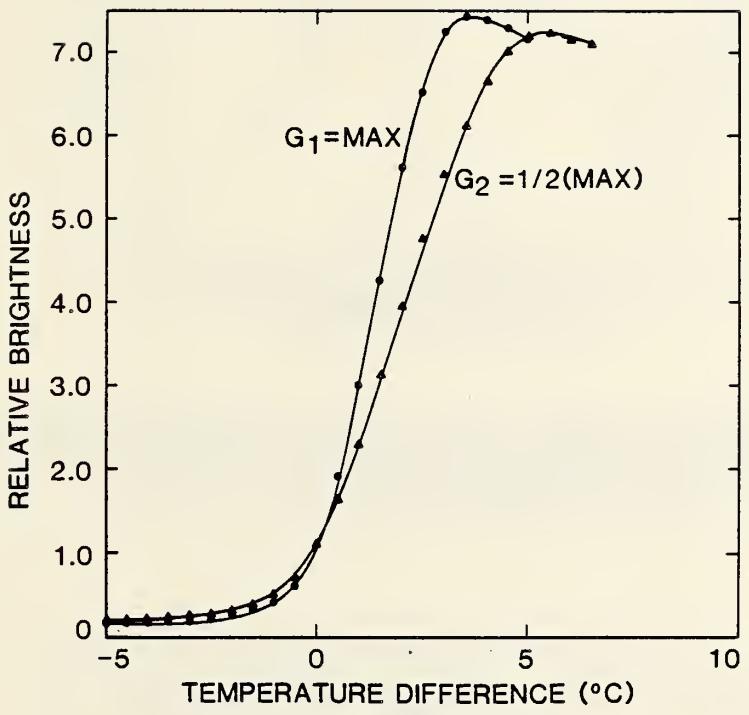

Figure 15c. Relative Brightness versus Temperature Difference from SiTF Test of System D at Maximum Thermal Level (Brightness) for two gains (Contrast)

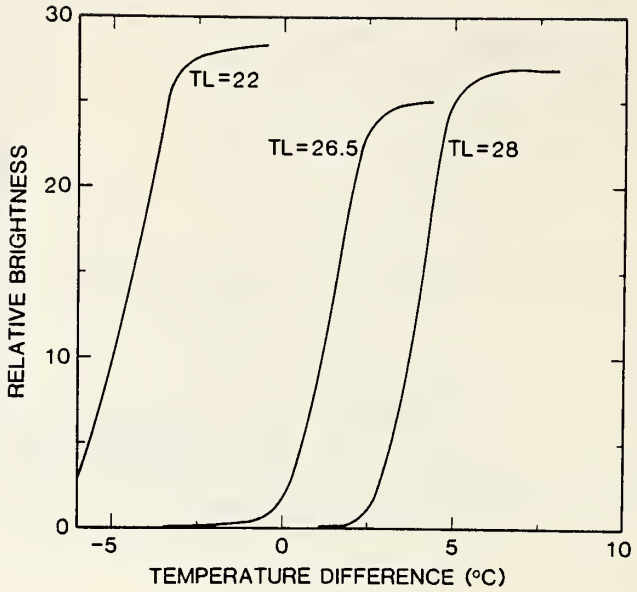

Figure 15d. Relative Brightness versus Temperature Difference from SiTF Test of System A at Constant Gain (S=2) for Various Thermal Levels

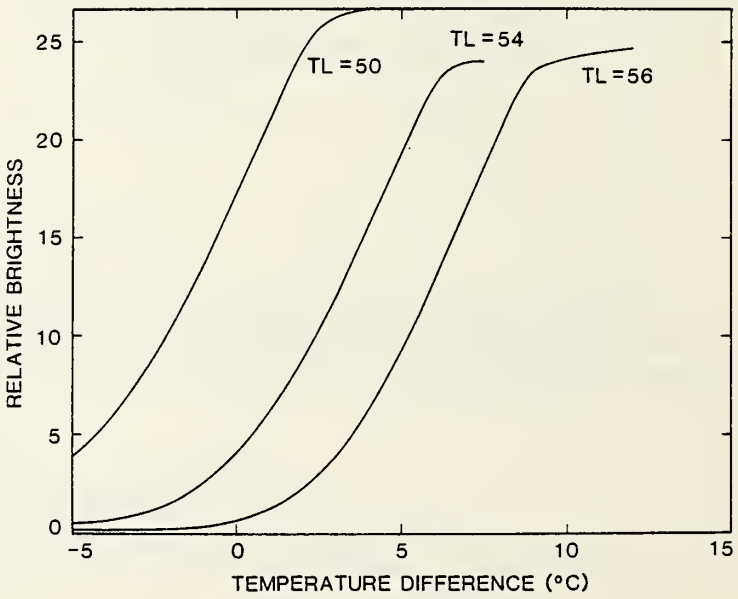

Figure 15e. Relative Brightness versus Temperature Difference from SiTF Test of System B at Constant Gain (S=5) for Various Thermal Levels

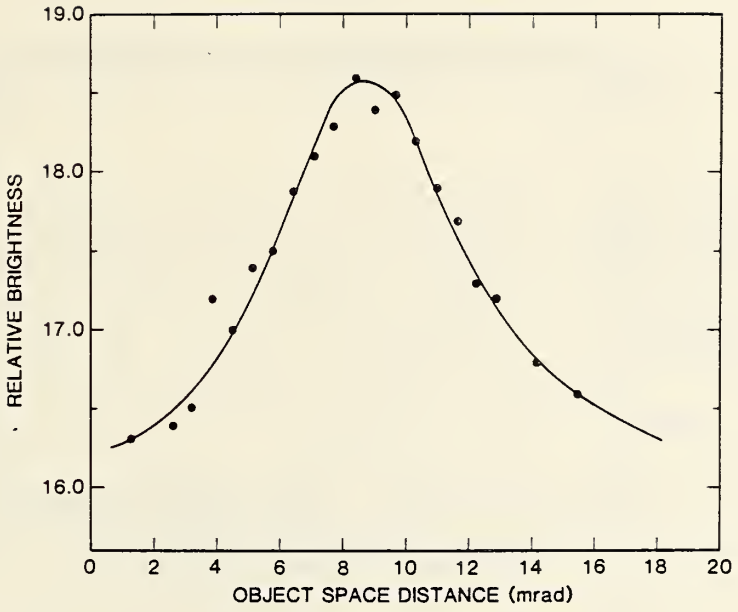

Figure 16a. Line Spread Function (LSF) of System A as a Function of Distance in Object Space (S=2, TL=26, and $\Delta T=18^{o}C$)

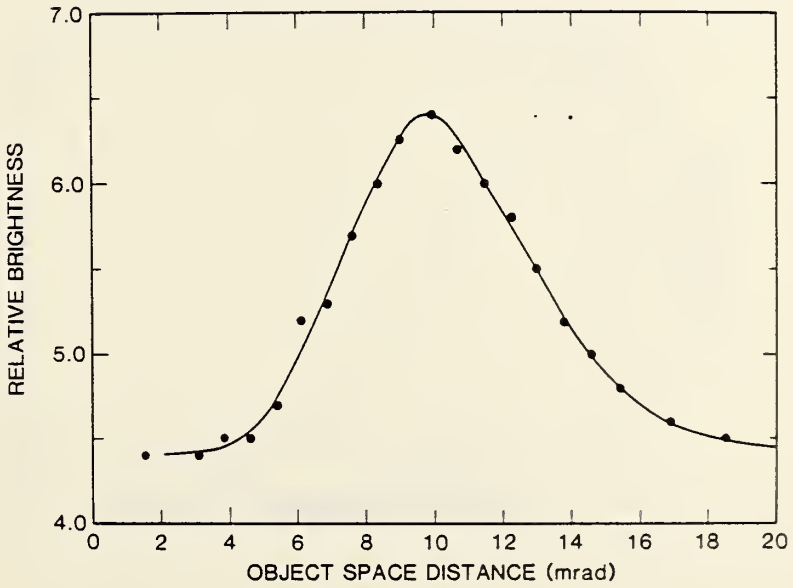

Figure 16b. Line Spread Function (LSF) of System B as a Function of Distance in Object Space (S=2, TL=54, and $\Delta T=15^{o}C$)

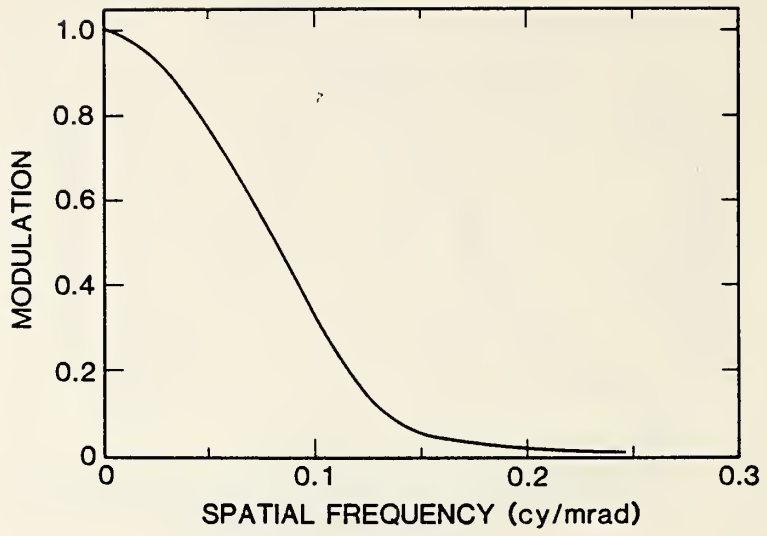

Figure 17a. Modulation Transfer Function (MTF) of System A as a Function of Object Space Frequency (S=2, TL=26, and $\Delta T=18^{o}C$)

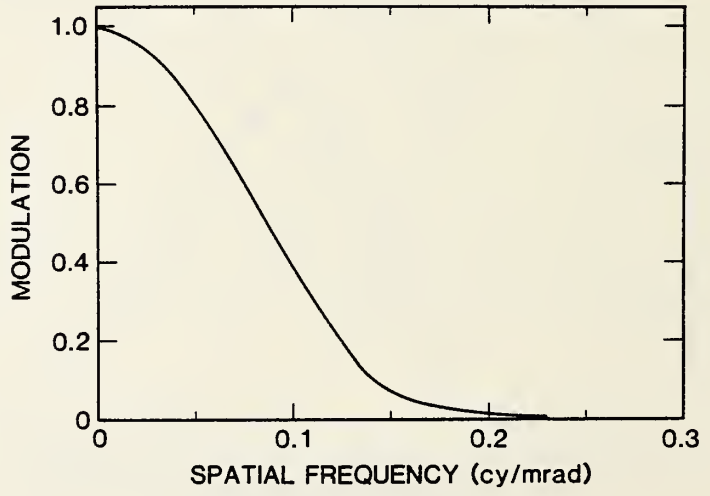

Figure 17b. Modulation Transfer Function (MTF) of System B as a Function of Object Space Frequency (S=2, TL=54, and $\Delta T=15^{o}C$)

APPENDIX

Material to be Built (or Modified) by NBS Machine Shop

This section includes detailed drawings of the components that are required to be constructed in-house by NBS. Figures A-1 to A-4 illustrate the Target Concept of Target Backgroung Plate with temperature probe holder, Target Pattern Holder, and Target Support Plate (items 7, 8, and 3 in figures 2 and 3). Figures A-5 to A-13 describe the Sliding Pattern Bracket and Seven Target Plates. Figures A-14 and A-15 give dimensions of the Target Source Table and the Sensor/Monitor Table (items 1 and 9 in figures 2 and 3). Figures A-16 and A-17 are drawings of the Sensor/Monitor Mounting Plate and the Optical Rail (items 11 and 14 in figures 2 and 3). The Optical Rail is currently available in NBS and need to be modified according to the descriptions. Figure A-18 is the Coupling Lens Holder. Figures A-19 and A-20 are the Source Mounting Block and the Sensor Mounting Block (item 4 and 12 in figures 2 and 3) which are rectangular blocks of wood cut to the desired heights for the Blackbody and various sensors. Figure A-21 gives the dimensions of the Remote Monitor Display Mounting Block and Mounting Plate (items 21 and 23 in figure 3) which are built to mount the Display Rotating Table (item 22 in figure 3). The Rotating Table is an existing item in NBS.

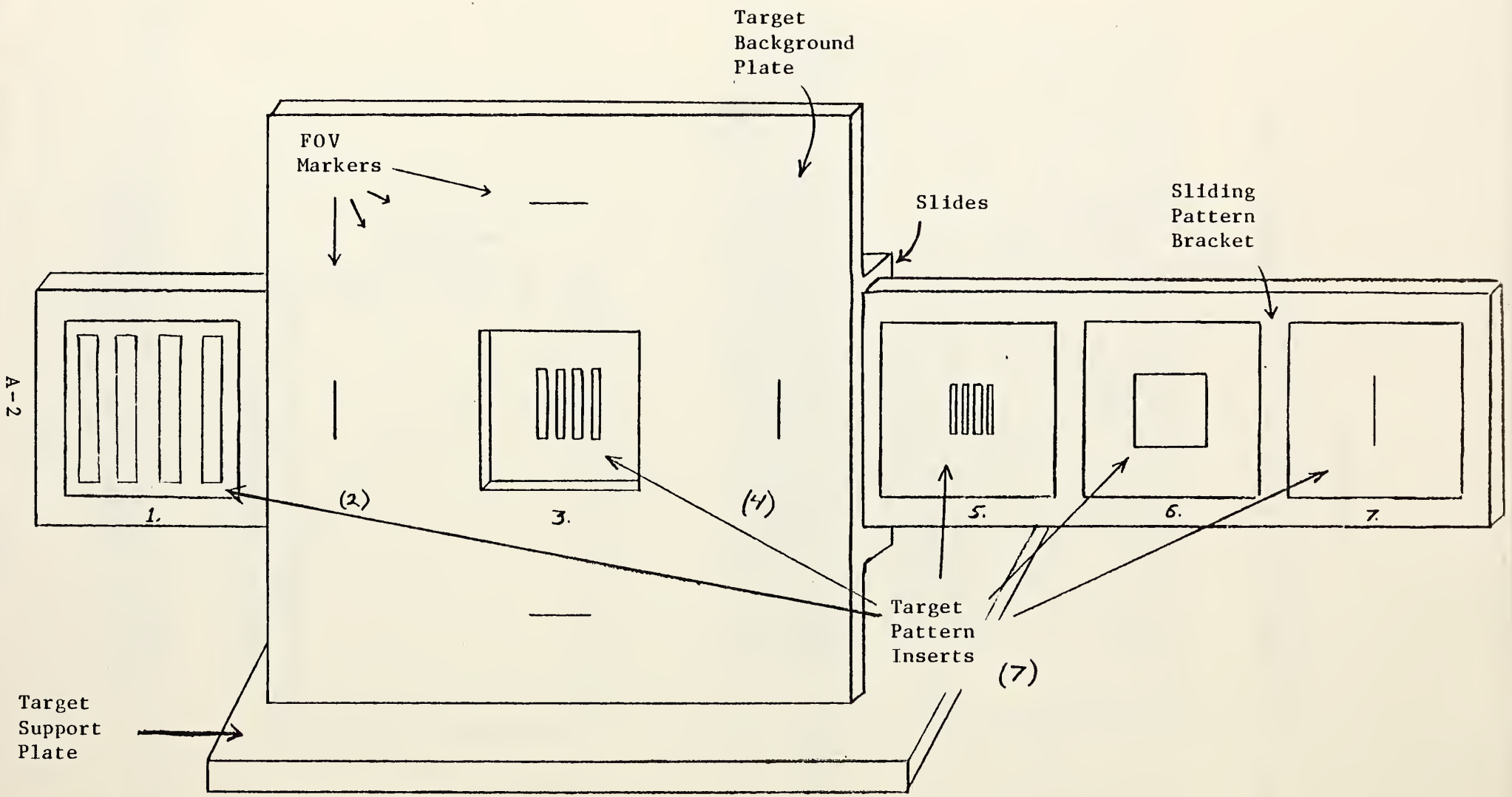

Figure A-1. Target Concept

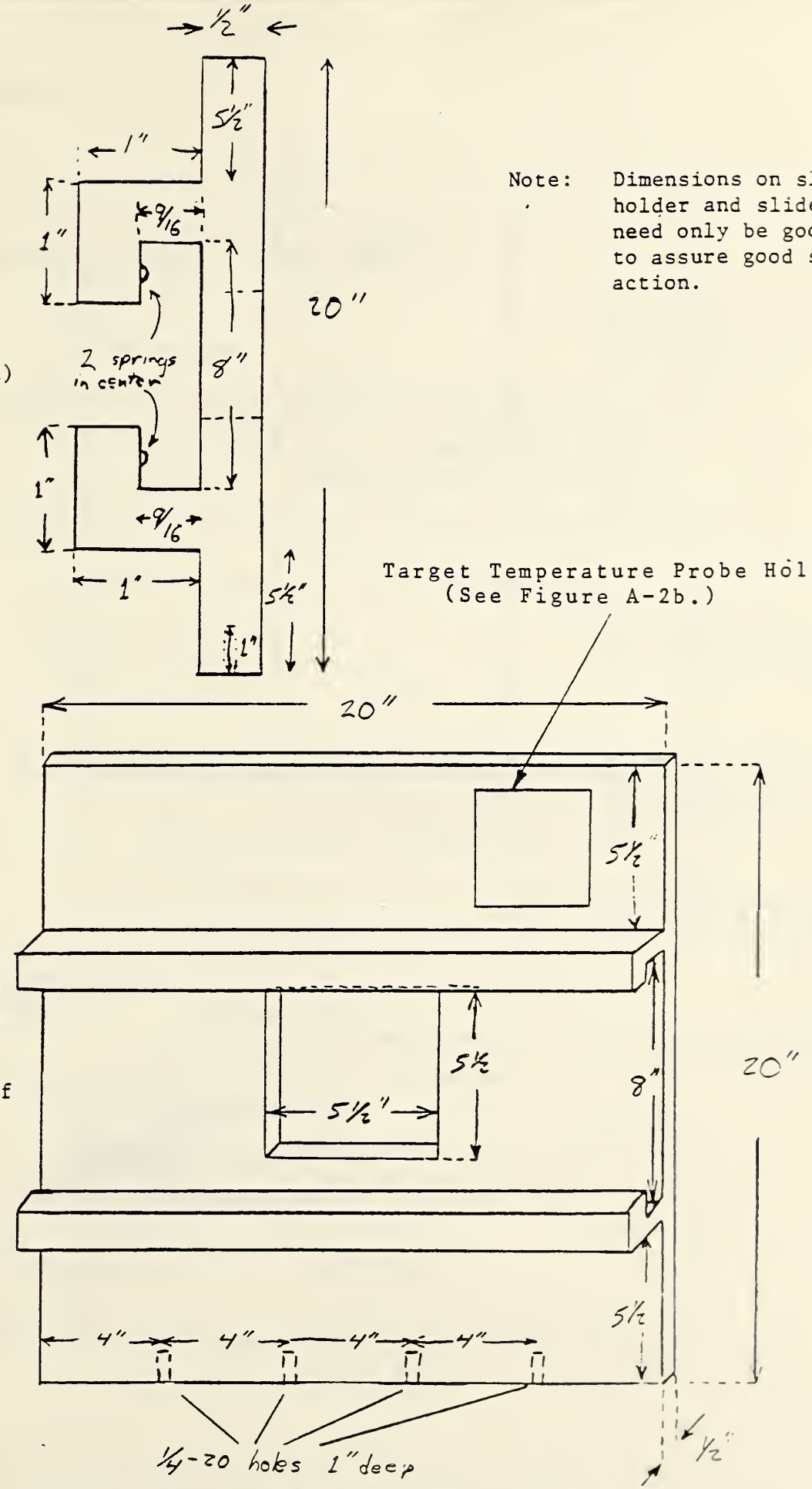

Note: Dimensions on slide holder and slide itself need only be good enough to assure good slide action.

Figure A-2a. Target Blackground Plate

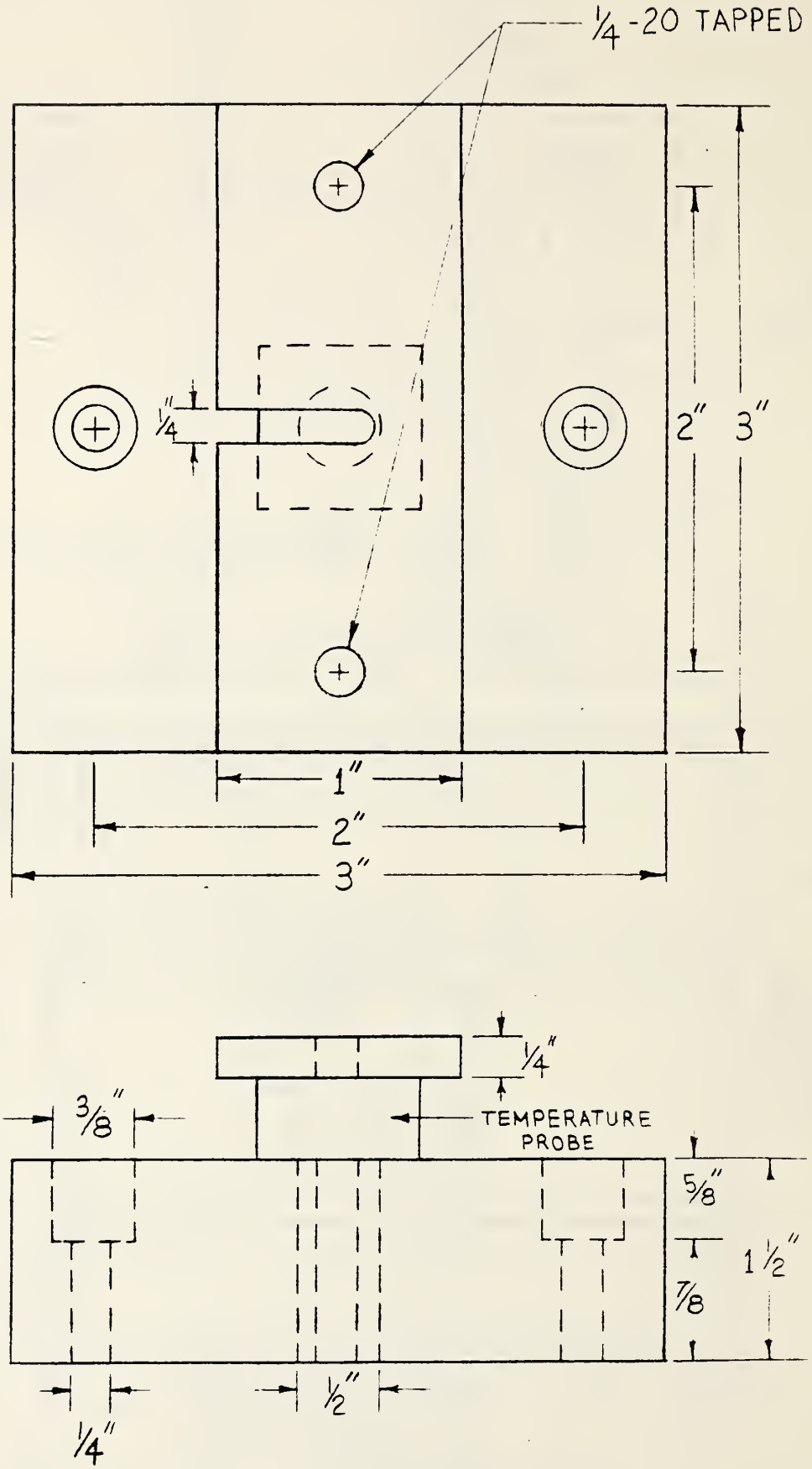

Figure A-2b. Target Temperature Probe Holder

Ball Detent Looking Down on Slide Holder Top-

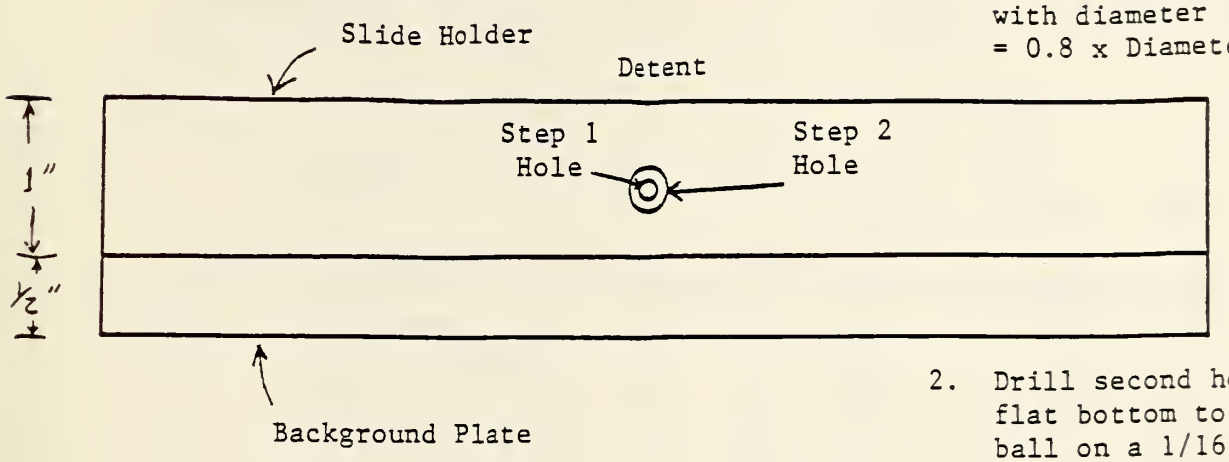

1. Drill all the way through with diameter = 0.8 x Diameter of Ball.

2. Drill second hole with flat bottom to hold ball on a 1/16" shelf.

3. Tap hole in step 2 to allow screw to hold retainer spring.

4. This may require adding additional material to top.

5. See side view concept.

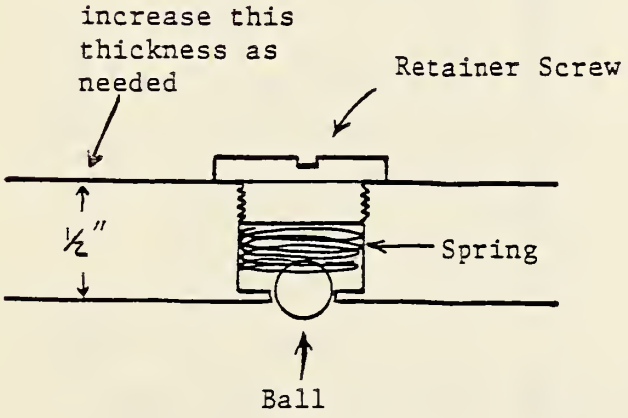

Figure A-3. Close-Up of Ball Detent

(all holes: 1/4 - 20)

i.e. 4- 1/4 - 20 screws will hold target plate to base plate: If angle iron is needed for stability, use it.

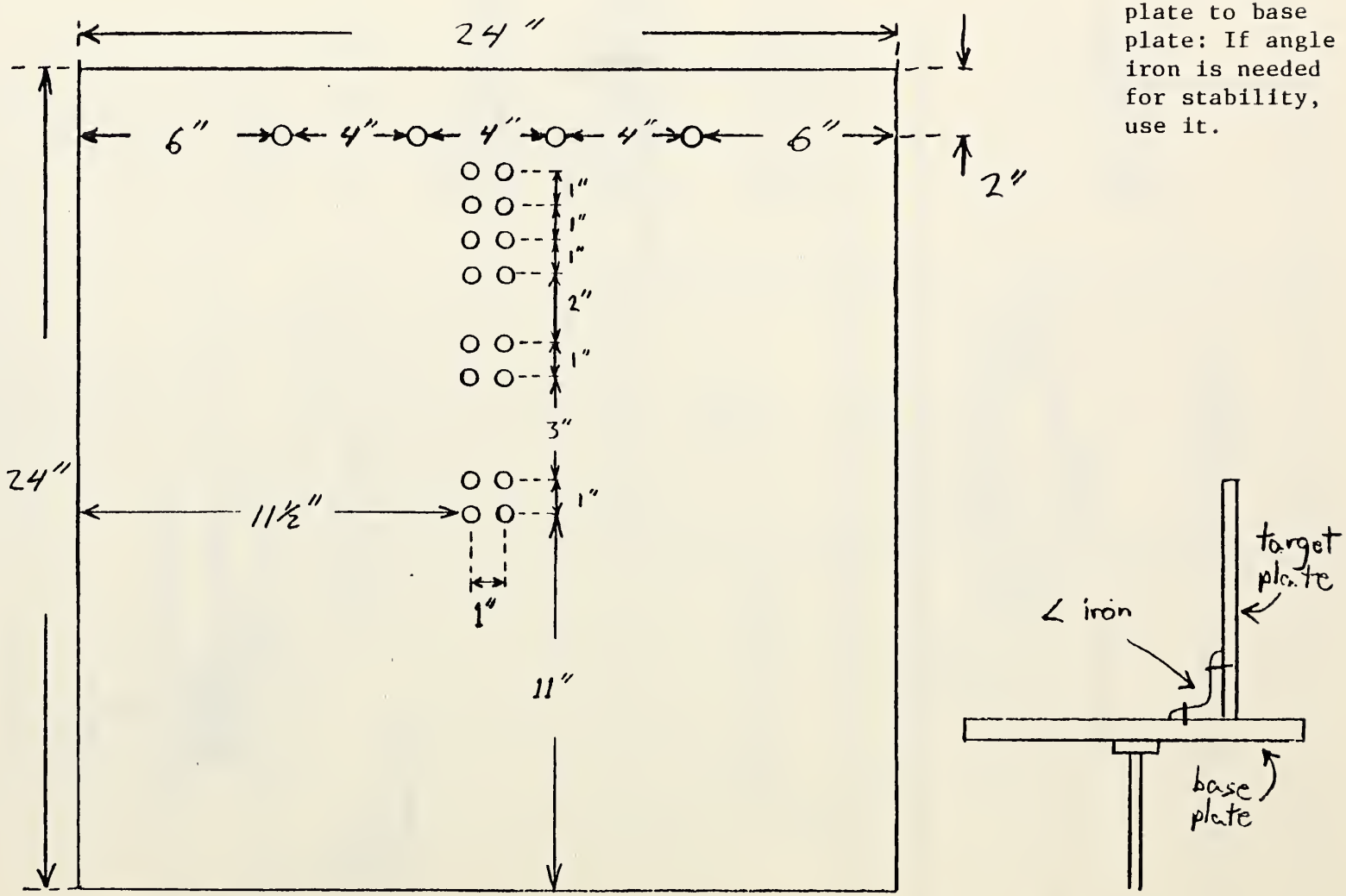

Figure A-4. Target Support Plate---1" Thickness

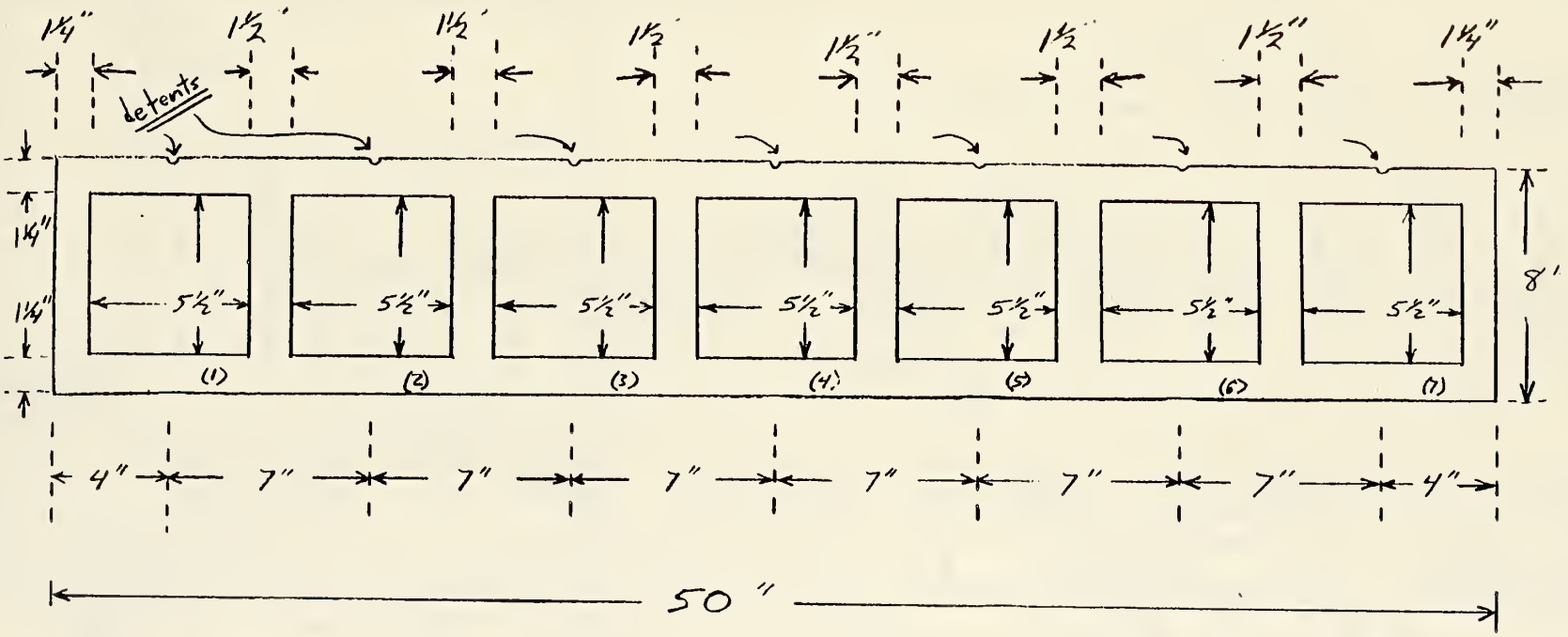

Tolerance: Keep openings at
5½" or slightly greater
- 0"
+ 0.1"

Figure A-5. Sliding Pattern Bracket (Front View)

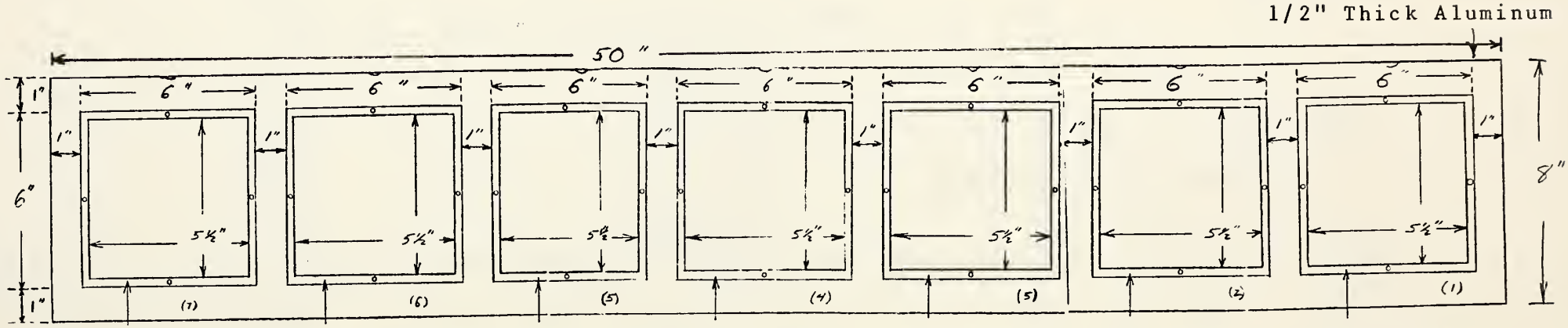

1/4" wide ledge sunk 3/16" all the way around 5.5" * 5.5" hole

1/4" ledge sunk 1/16"

1/4" ledge sunk 3/16"

1/4" ledge sunk 1/8"

1/4" ledge sunk 1/8"

1/4" ledge sunk 3/16"

1/4" ledge sunk 1/8"

(Each 1/4" ledge has a screw hole sunk in the center)

Figure A-6. Sliding Pattern Bracket (Rear View)

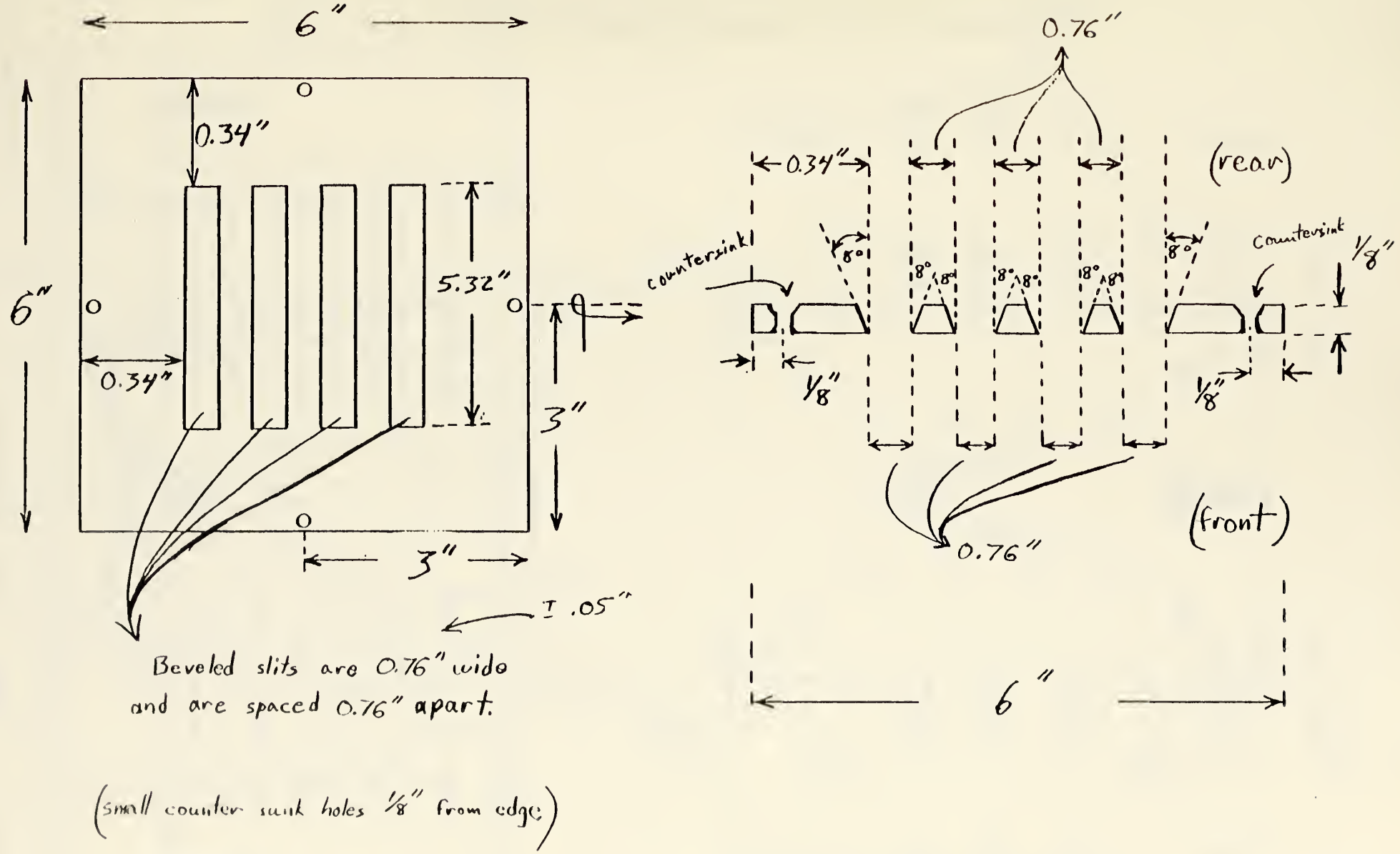

Front View

Top View of Center Cross-section

Figure A-7. Target Pattern Plate #1---1/8" Thickness

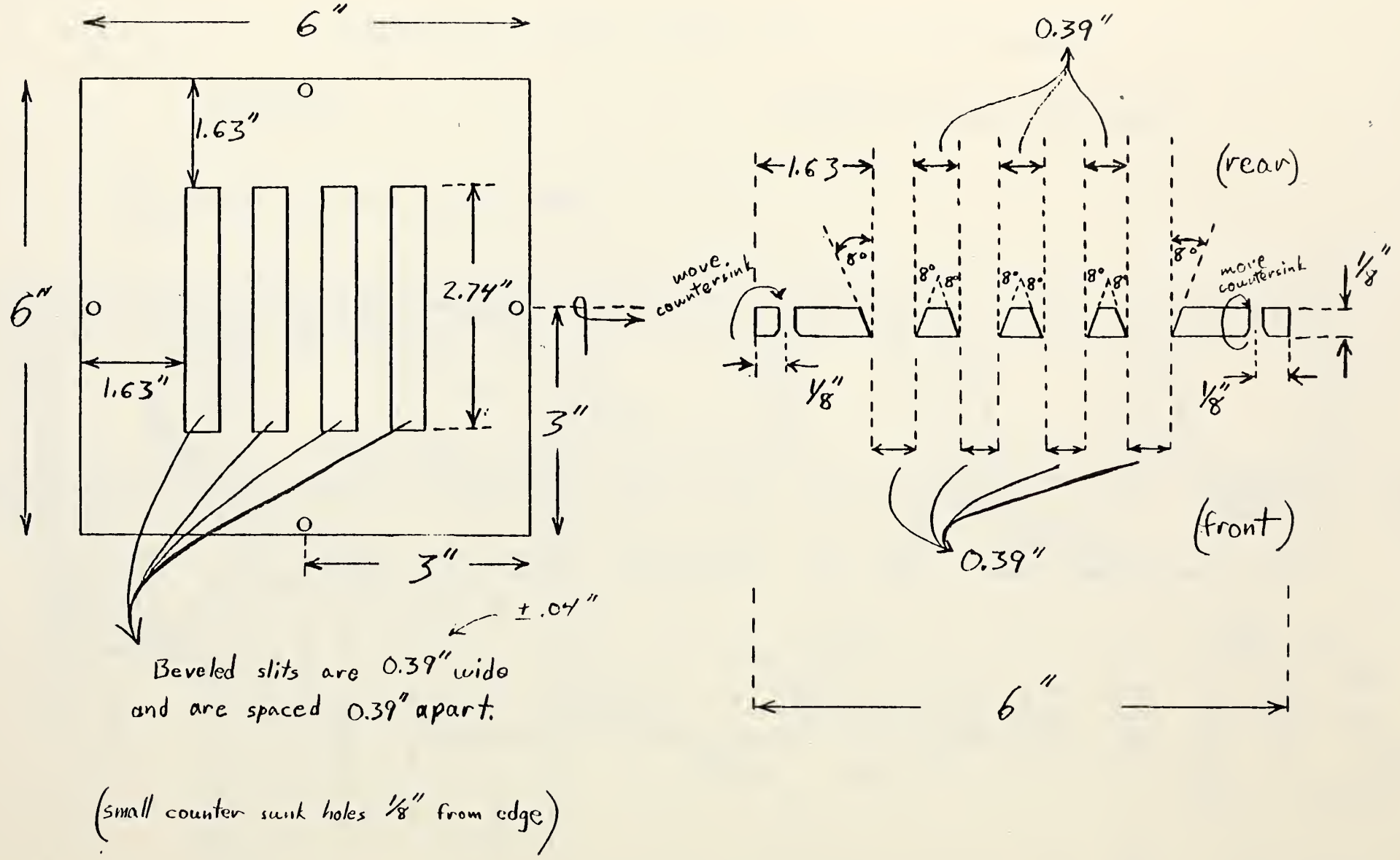

Figure A-8. Target Pattern Plate #2---1/8" Thickness

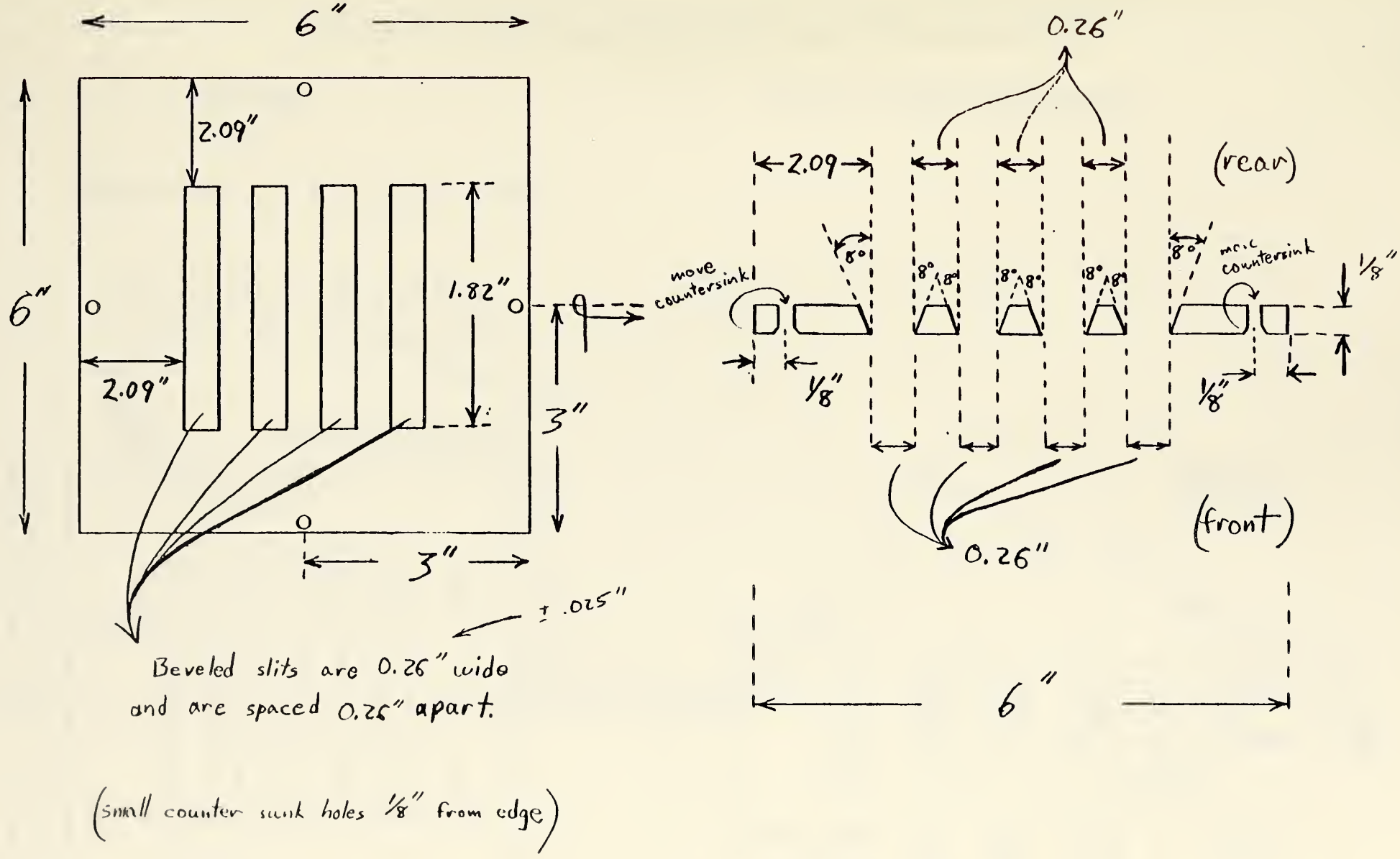

Front View

Top View of Center Cross-section

Figure A-9. Target Pattern Plate #3---1/8" Thickness

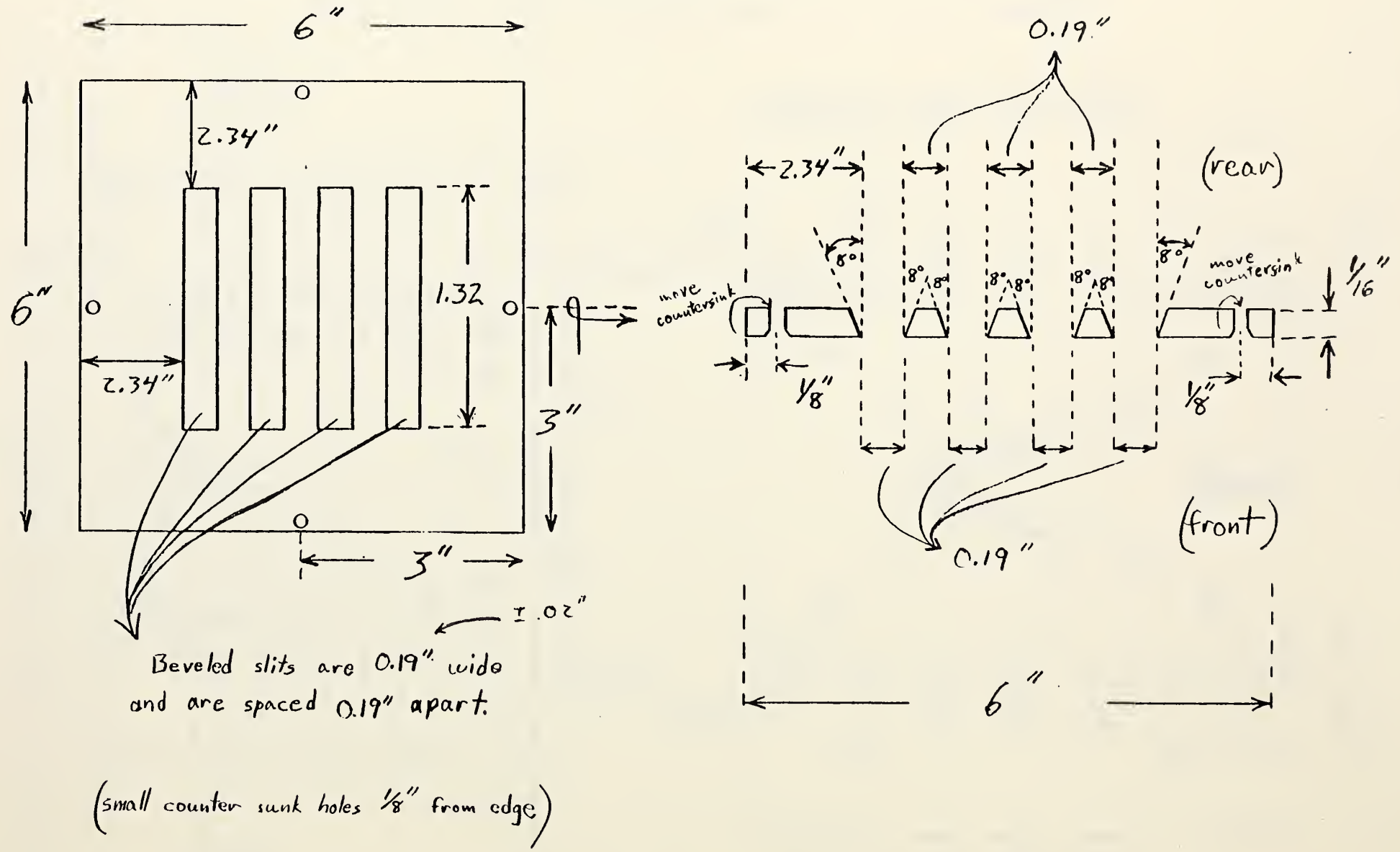

Figure A-10. Target Pattern Plate #4---1/16" Thickness

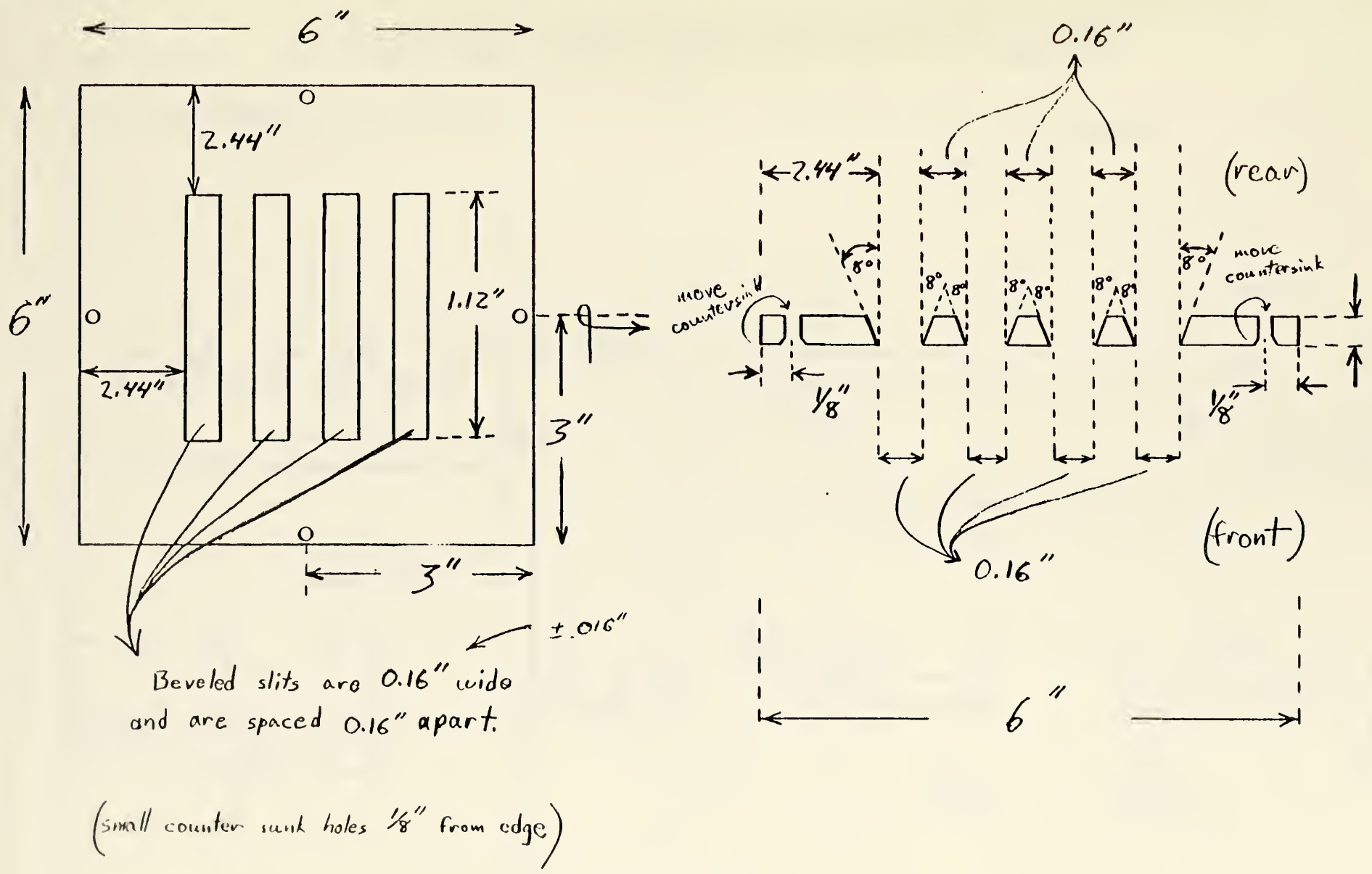

Front View

Top View of Center Cross-section

Figure A-11. Target Pattern Plate #5---1/16" Thickness

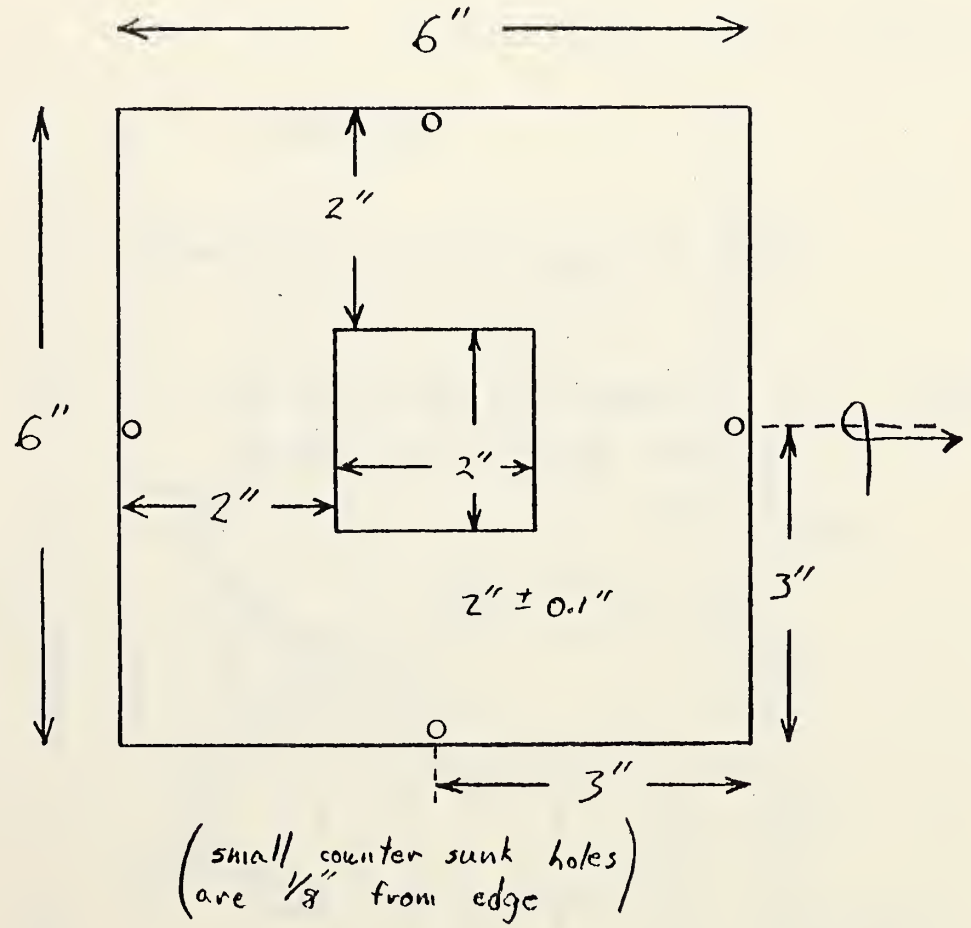

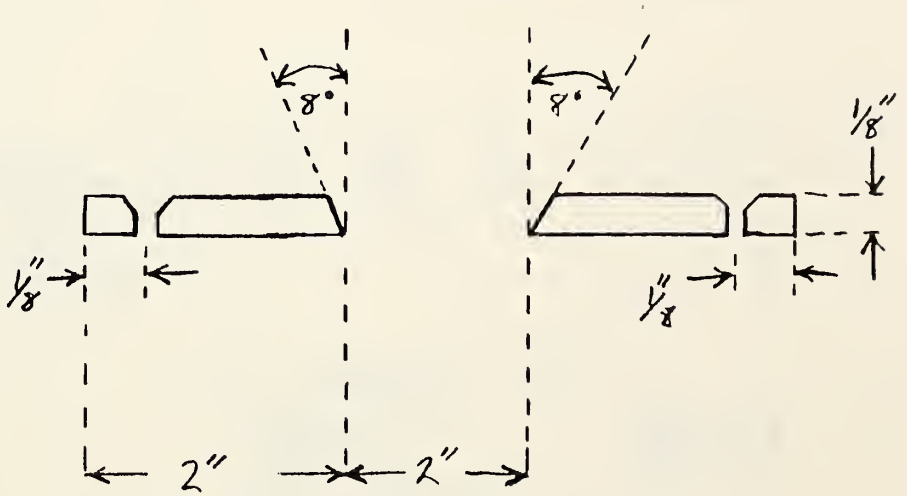

Front View

Top View of Center Cross-section

Figure A-12. Target Pattern Plate #6---1/8" Thickness

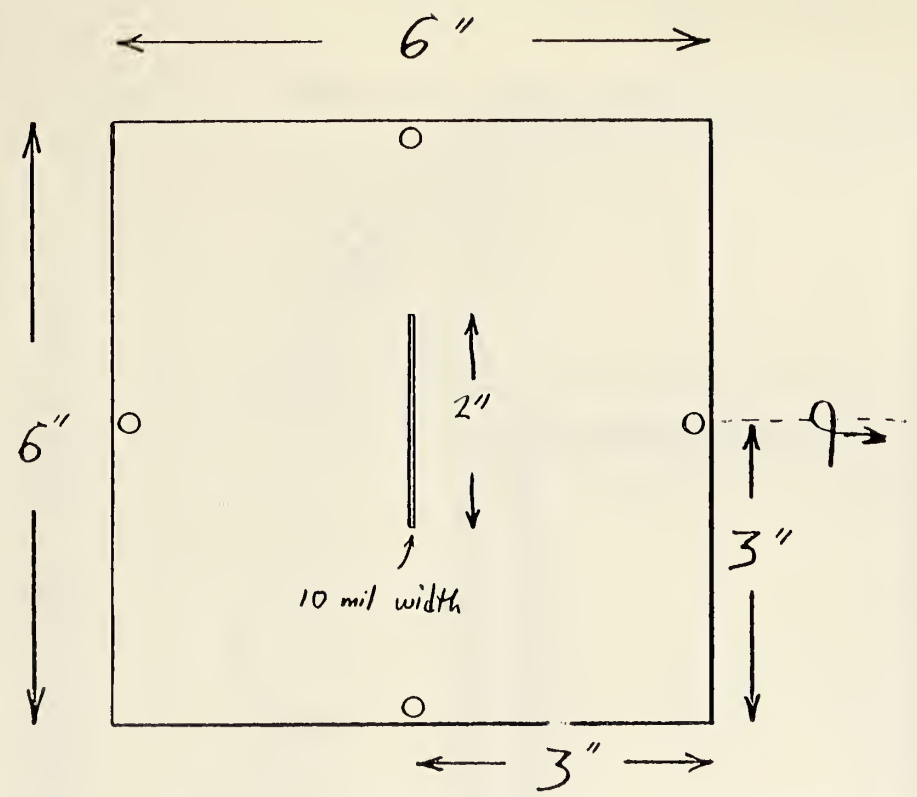

Front View

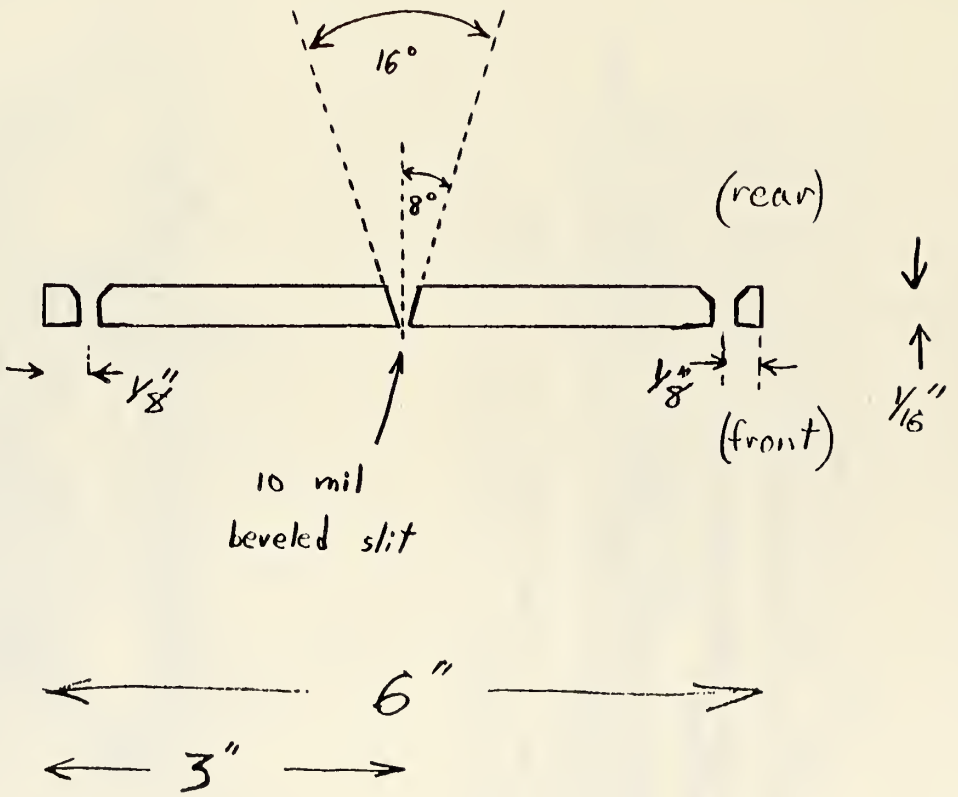

Top View of Center Cross-section

Figure A-13. Target Pattern Plate #7---1/16" Thickness

1. Angle iron solid construction of frame.
2. Cover with thin sheet metal stock. (Paint to suit.) (Not shown here.)
3. Center plate on top must support solid 200-300 lbs. (½" thick aluminum or steel, hole spacings to fit model 2501 jactuator)
4. Hole spacings on bottom corners to fit model 4-30-113P-2 casters. (2 with brakes, 2 without)

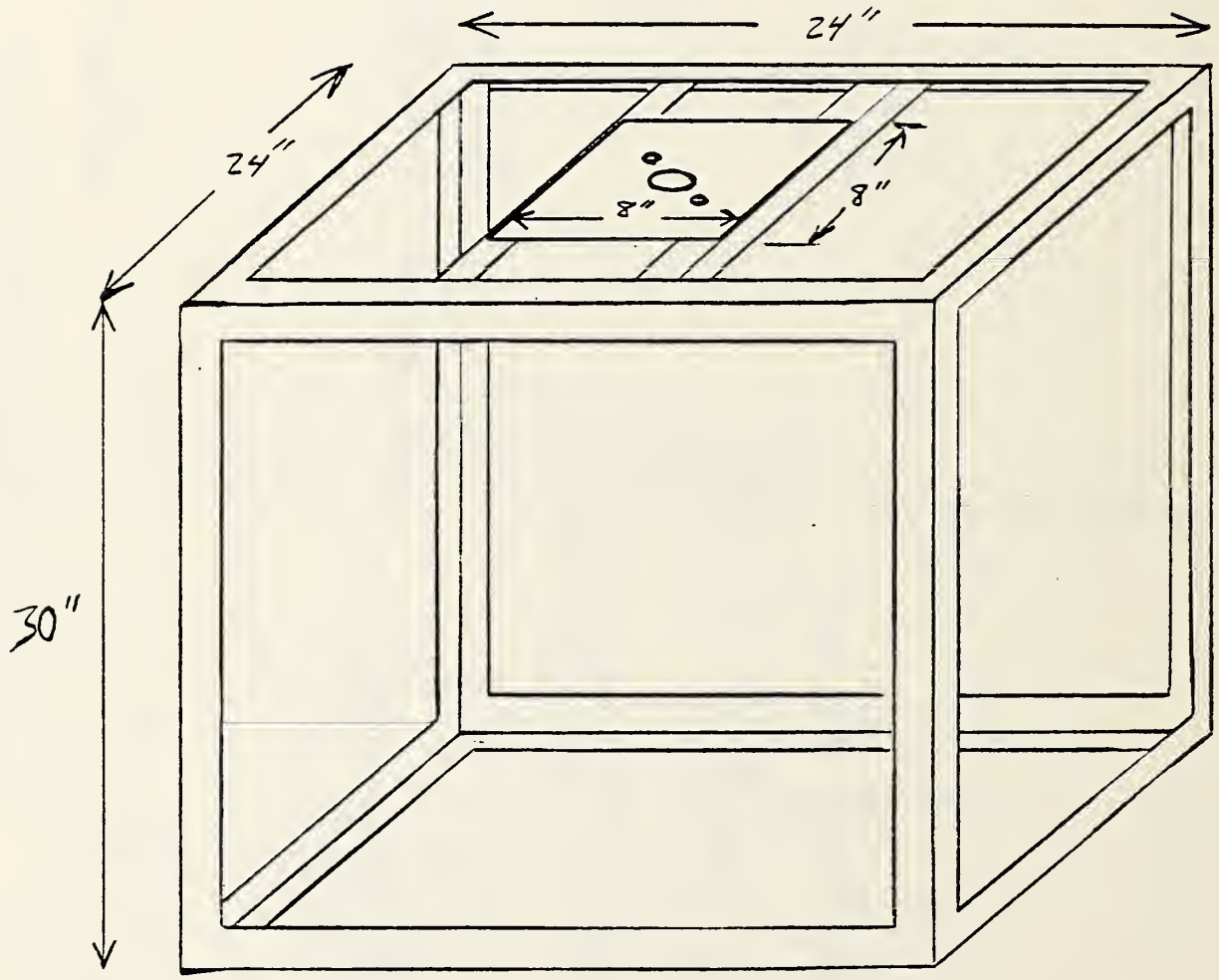

Figure A-14. Source Table

1. Angle iron solid construction of frame.
2. Cover with thin sheet metal stock. (Paint to suit.) (Not shown here.)
3. Center plate on top must support 500 lbs. (3/4" thick aluminum or steel)
4. Hole spacings on bottom corners to fit model 4-30-113P-2 casters. (2 with brakes, 2 without)

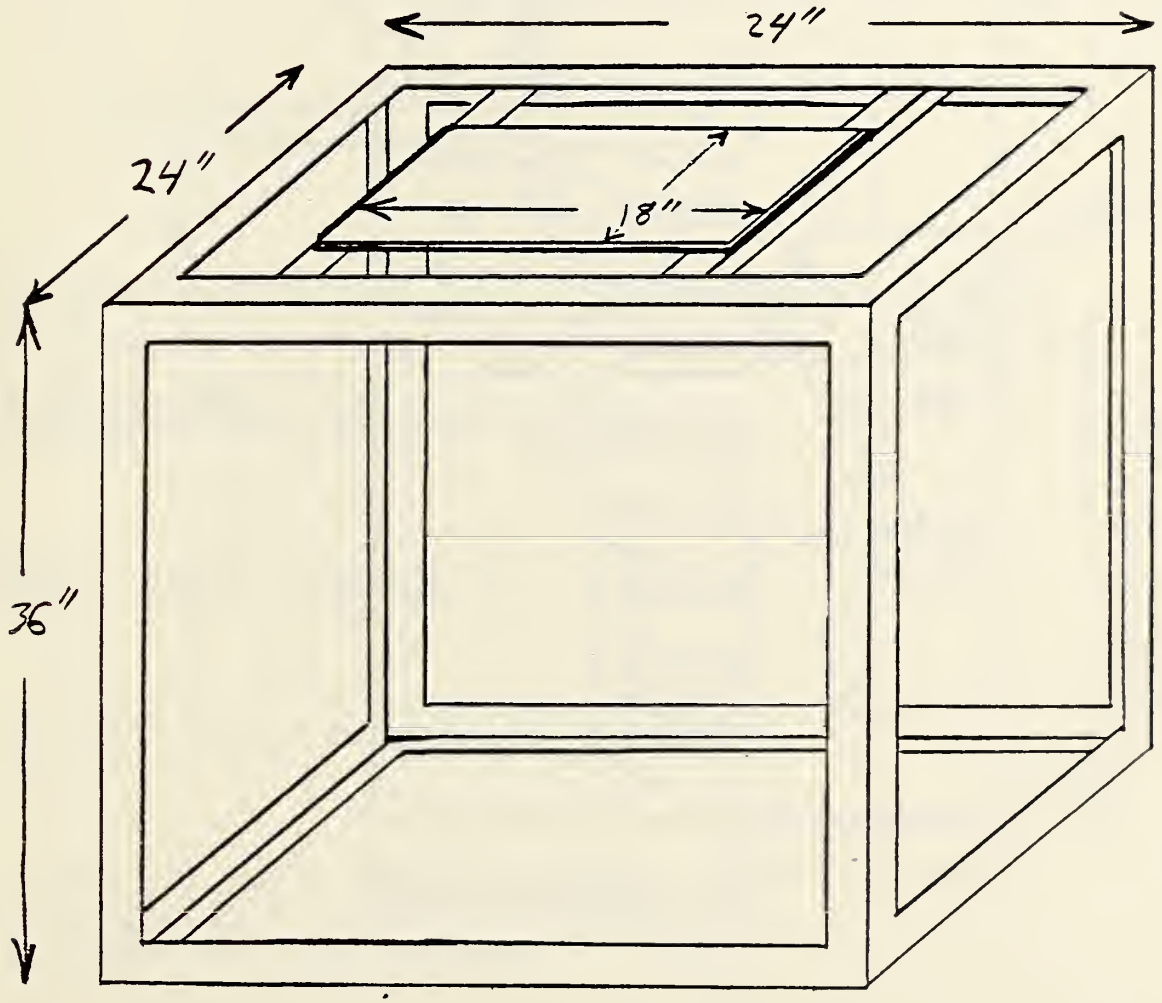

Figure A-15. Sensor/Monitor Table

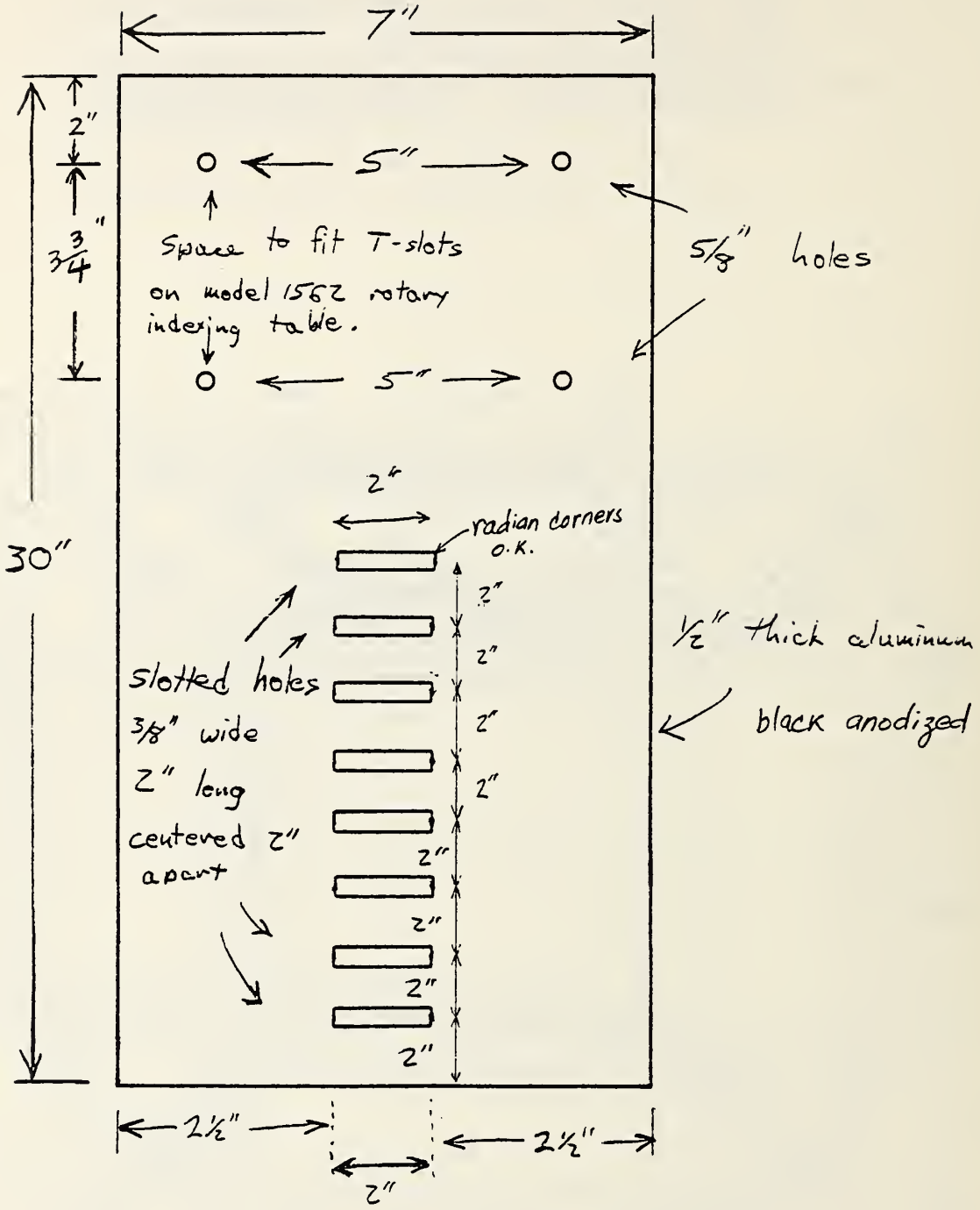

Figure A-16. Sensor/Monitor Mounting Plate

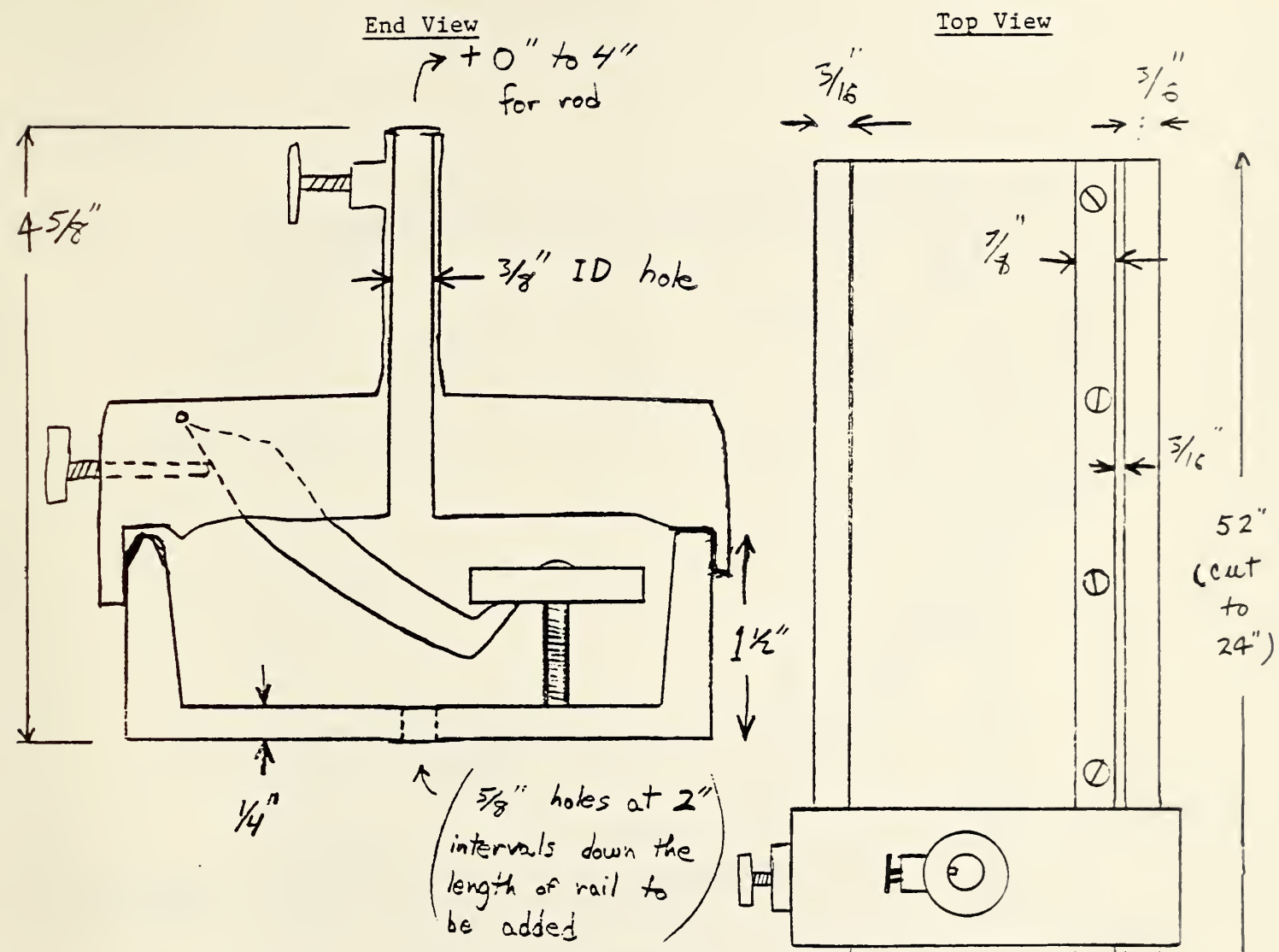

Shop work needed:

1.) Cut rail to a length of 24".

2.) Drill 5/8" holes through bottom at 2" intervals.

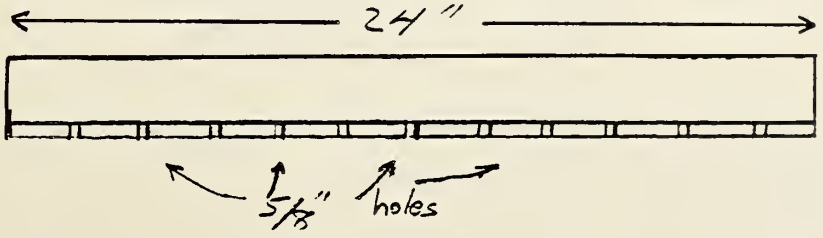

Figure A-17. Optical Rail

(Not To Scale)

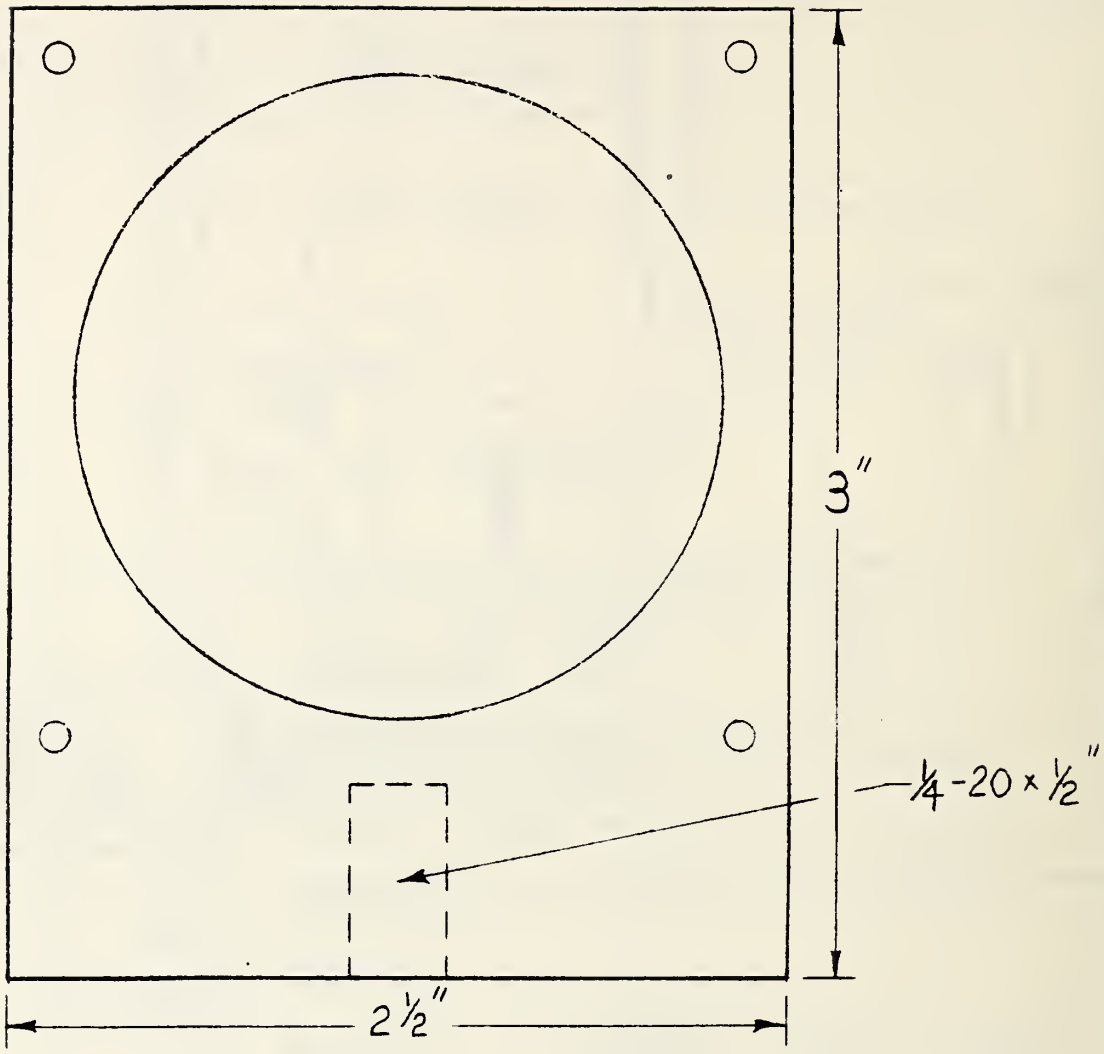

½" THICK ALUMINUM

4 HOLES TAPPED 2-56 × 5/16"

Figure A-18. Coupling Lens Holder

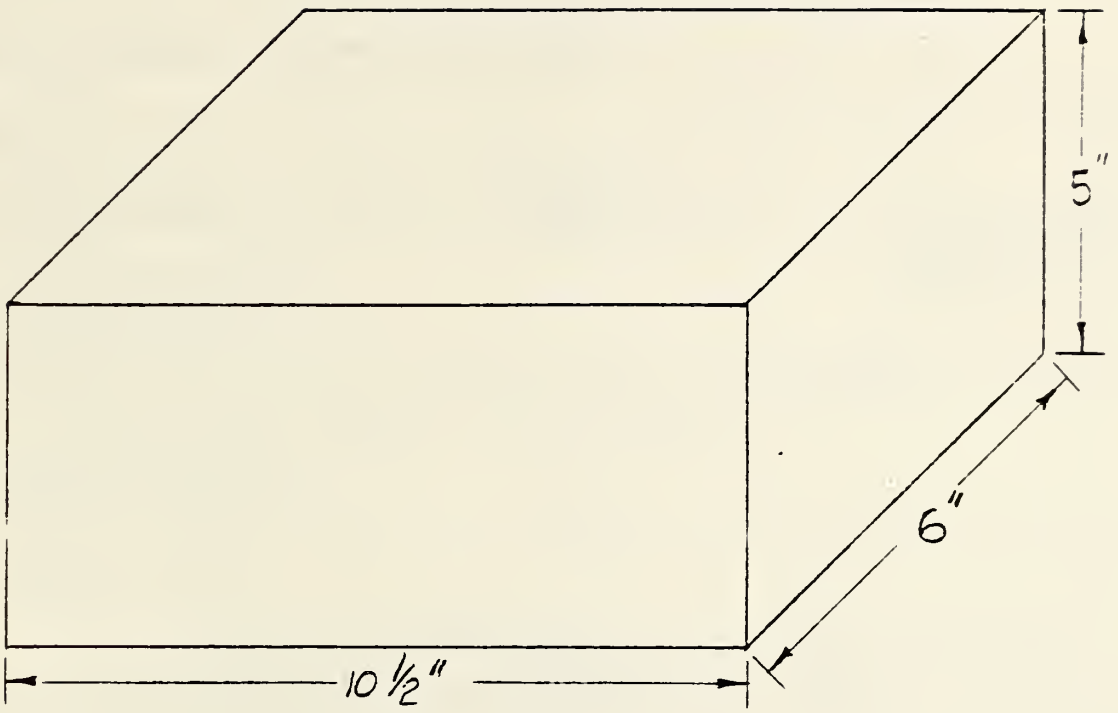

Figure A-19. Source Mounting Block

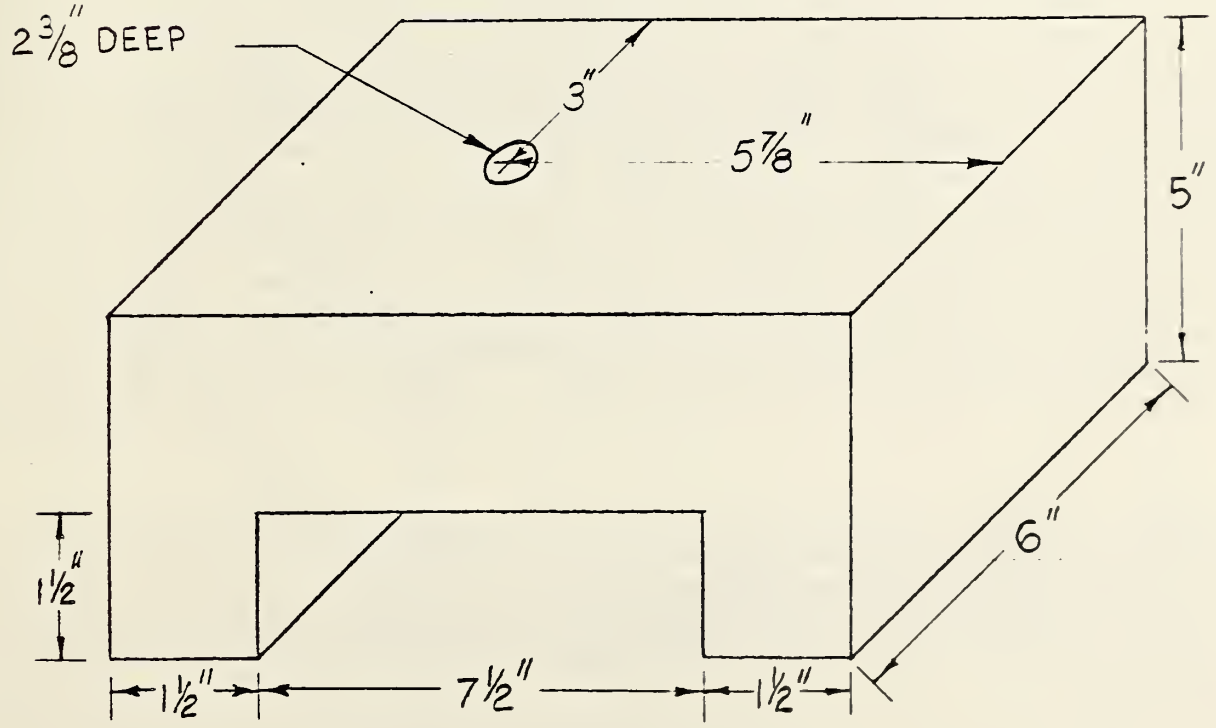

Figure A-20. Sensor Mounting Block

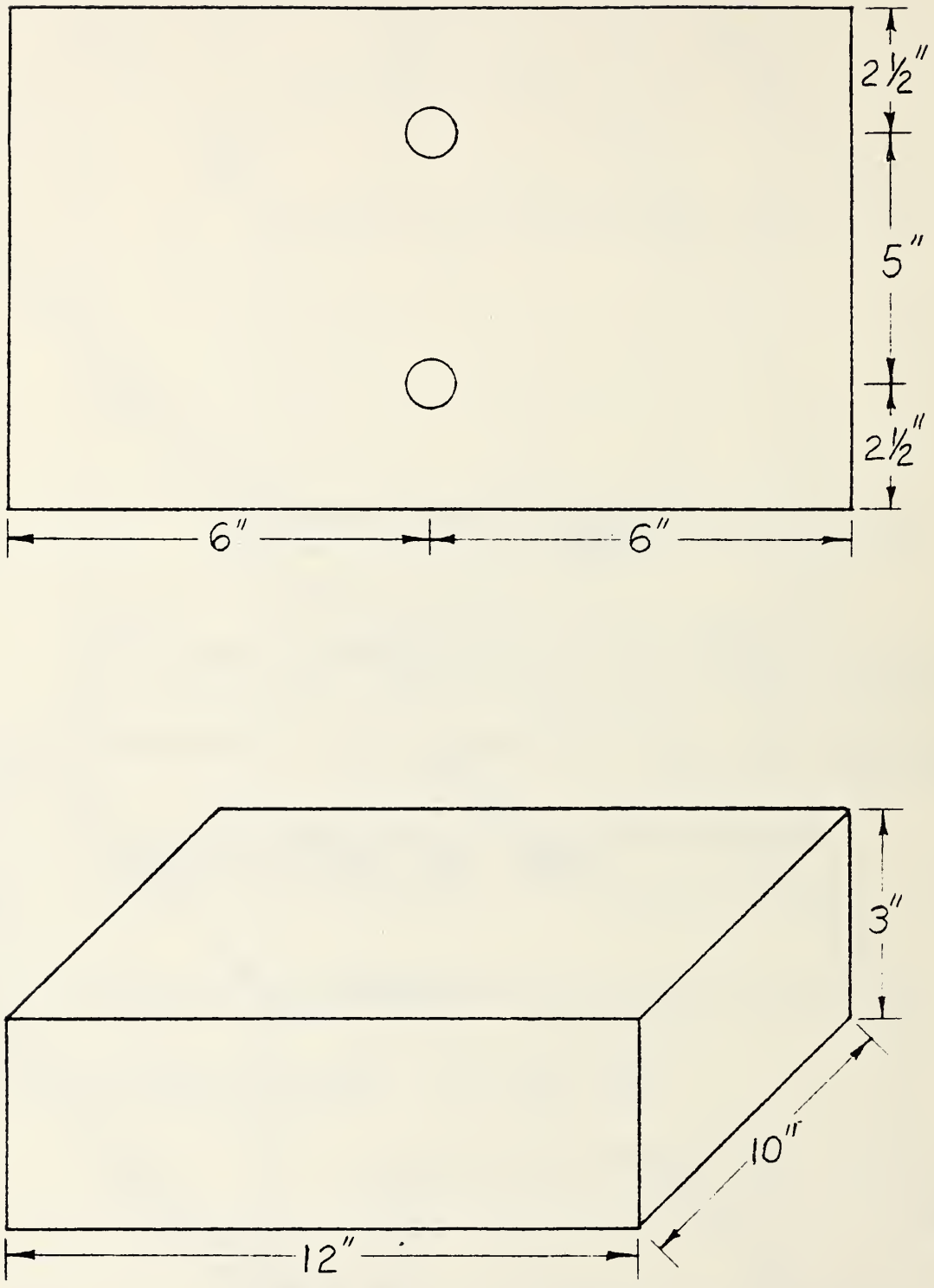

Figure A-21. Remote Monitor Display Mounting Plate and Block

FORM NBS-114A (REV. 11-84)

U.S. DEPT. OF COMM. BIBLIOGRAPHIC DATA SHEET (See instructions)	1. PUBLICATION OR REPORT NO. NBSIR 85-3131	2. Performing Organ. Report No.	3. Publication Date June 1985

4. TITLE AND SUBTITLE

Laboratory Design and Test Procedures for Quantitative Evaluation of Infrared Sensors to Assess Thermal Anomalies

5. AUTHOR(S)

Y. May Chang, Richard A. Grot and James T. Wood

6. PERFORMING ORGANIZATION (If joint or other than NBS, see instructions)

NATIONAL BUREAU OF STANDARDS
U.S. DEPARTMENT OF COMMERCE
GAITHERSBURG, MD 20899

7. Contract/Grant No. Interagency Agreement DEAI-01-76

8. Type of Report & Period Covered

9. SPONSORING ORGANIZATION NAME AND COMPLETE ADDRESS (Street, City, State, ZIP)

Office of Building Energy Research and Development
U.S. Department of Energy
Washington, DC 20585

10. SUPPLEMENTARY NOTES

☐ Document describes a computer program; SF-185, FIPS Software Summary, is attached.

11. ABSTRACT (A 200-word or less factual summary of most significant information. If document includes a significant bibliography or literature survey, mention it here)

This report presents the description of the laboratory apparatus and preliminary results of the quantitative evaluation of three high-resolution and two low-resolution infrared imaging systems. These systems which are commonly used for building diagnostics are tested under various background temperatures (from -20°C to 25°C) for their minimum resolvable temperature differences (MRTD) at spatial frequencies from 0.03 to 0.25 cycles per milliradian. The calibration curves of absolute and differential temperature measurements are obtained for three systems. The signal transfer function and line spread function at ambient temperature of another three systems are also measured. Comparisons of the dependence of the MRTD on background temperatures from the measured data with the predicted values given in ASHRAE Standards 101-83 are also included. The dependence of background temperatures for absolute temperature measurements are presented, as well as comparison of measured data and data given by the manufacturer. Horizontal on-axis magnification factors of the geometric transfer function of two systems are also established to calibrate the horizontal axis for the measured line spread function to obtain the modulation transfer function. The variation of the uniformity for horizontal display of these two sensors are also observed. Included are detailed descriptions of laboratory design, equipment setup, and evaluation procedures of each test.

12. KEY WORDS (Six to twelve entries; alphabetical order; capitalize only proper names; and separate key words by semicolons)

Background temperature; calibration curves; display uniformity; infrared sensing systems; laboratory evaluation; line spread function; magnification factor; minimum resolvable temperature difference; modulation transfer function; signal transfer function; spatial frequency; target temperature

13. AVAILABILITY

☒ Unlimited

☐ For Official Distribution. Do Not Release to NTIS

☐ Order From Superintendent of Documents, U.S. Government Printing Office, Washington, DC 20402.

☒ Order From National Technical Information Service (NTIS), Springfield, VA 22161

14. NO. OF PRINTED PAGES 85

15. Price $11.50

USCOMM-DC 6043-P80